Department of Biomedical Science
University of Veterinary Medicine Vienna

Pharmacology and Toxicology Division
(Head: O.Univ.-Prof. Dr.med.vet. Mathias M ller)

Sterol endoperoxides: Influence on *Leishmania* and macrophages

Bachelor thesis

University of Veterinary Medicine Vienna

Submitted by

Azra Aleta

Vienna, June 2024

All experiments for this thesis were conducted from February to May 2023 under the supervision of Ao. Univ.-Prof. Dr.rer.nat. Lars Gille at the Pharmacology and Toxicology Division in the Department of Biomedical Sciences.

Reviewer: Dipl.-Biol. Dr.rer.nat. Rudolf Moldzio
Department of Biomedical Sciences
Medical Biochemistry Division
University of Veterinary Medicine Vienna
Veterinärplatz 1
1210 Vienna

Acknowledgements

First and foremost, I would like to extend my gratitude to Ao.Univ.-Prof. Dr.rer.nat. Lars Gille for his invaluable guidance and patience throughout my thesis, consistently encouraging me and providing his expertise.

Furthermore, I would like to appreciate everyone at the Pharmacology and Toxicology Divison, especially Ao.Univ.-Prof. Dr. rer.nat. Katrin Staniek, for creating such a great work environment in my time there.
Additionally, I would like to thank Dipl.-Biol. Dr.rer.nat. Rudolf Moldzio for reviewing this thesis.

Lastly, I want to extend my heartfelt thanks to my family and friends for their unwavering support and understanding throughout this process.

Table of Contents

1. Introduction

1.1 Leishmaniasis

Leishmania, intracellular protozoan parasites, are responsible for causing a tropical disease called leishmaniasis (McGwire and Satoskar 2014). Leishmaniasis affects people in tropical and subtropical regions reaching from Africa and Asia to North and South America as well as Europe (Alven and Aderibigbe 2020).
With its impact spanning 98 countries and affecting at least two million individuals annually, while posing a threat to 350 million, leishmaniasis is recognized as a neglected tropical disease by the World Health Organization and therefore, considered a global health issue (McGwire and Satoskar 2014).

Clinically, there are three main manifestations: cutaneous, mucocutaneous and visceral leishmaniasis (Handler et al. 2015). The most abundant form is cutaneous leishmaniasis, being not lethal but leaving permanent wounds and ulcerations that often lead to stigmas and mental health problems in patients (Gurel et al. 2020).
After a previous infection with the cutaneous form, mucocutaneous leishmaniasis can occur and result in nasal and oral cavities being destroyed. In most cases, mucocutaneous leishmaniasis occurs within two years of infection with cutaneous leishmaniasis but it can also develop decades later. The visceral form of leishmaniasis affects internal organs such as the liver, bone marrow or spleen, causing different symptoms, from fever to weight loss. With a mortality rate of 10 %, visceral leishmaniasis is in second place after malaria as the deadliest tropical parasitic disease. It is typically connected with *L. donovani*, *L. infantum* or *L. chagasi* (Handler et al. 2015).
As a complication patients with visceral leishmaniasis can also develop cutaneous leishmaniasis, known as post-kala-azar dermal leishmaniasis (Handler et al. 2015). The complication appears due to an immunological reaction to *Leishmania* residing within the skin (Pace 2014).

Due to numerous risk factors such as climate change and environmental conditions, population migration or low socioeconomic statuses of families, leishmaniasis occurs in various regions and its incidence is rising. Leishmaniasis coexisting with HIV or other diseases associated with immunosuppressed people is considered the main reason for the increasing cases of

cutaneous and visceral leishmaniasis in the Mediterranean region of Europe.
Moreover, dogs are shown to be possible reservoirs of *L. infantum* and play a key role in infection since they are household pets (Valero and Uriarte 2020).

1.1.1 Life cycle of *Leishmania*

Leishmania have a digenetic life cycle including two hosts, mammals and insects, and morphological differentiation, amastigotes and promastigotes (Sasidharan and Saudagar 2021).

In general, transmission of leishmaniasis is mediated by female phlebotomine sand flies. In the sand fly stage, *Leishmania* are found as motile flagellated promastigotes, whereas intracellular non-flagellated amastigotes appear in the human stage (McGwire and Satoskar 2013). While the promastigotes are adjusted for existence in the sand fly gut, the amastigotes are adapted for prevailing inside the mammalian host (Gluenz et al. 2010).

Whenever an infected sand fly bites a human or an animal, the *Leishmania* parasites, including microbiota and salivary proteins of the sand fly, are injected into the host skin, which can lead to the development of the disease (Serafim et al. 2020). The promastigotes are then transmitted to the host while causing a phagocytic process that enables them to access the macrophages and infect them (Fig. 1). In the parasitophorous vacuole of the macrophages, the promastigotes transform into amastigotes (Sasidharan and Saudagar 2021). The amastigotes are released through cell lysis and subsequently infect other macrophages. After another blood meal and ingestion by the sand fly, the amastigotes differentiate back to the promastigote form, and the cycle is completed (Pace 2014).

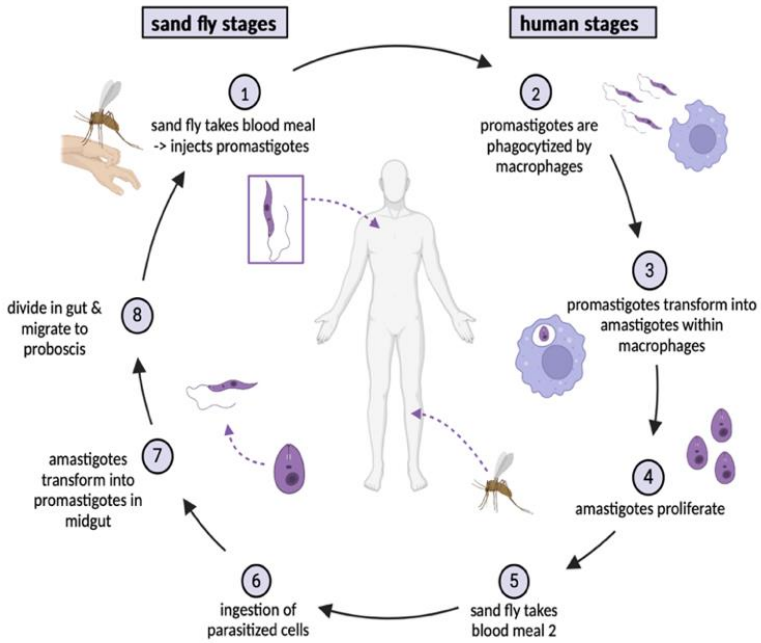

Figure 1: *Life cycle of Leishmania. (1) Sand fly injects the promastigotes (infective stage) into the host by taking a blood meal. (2) Promastigotes are phagocytized by host macrophages. (3) Promastigotes transform into amastigotes within the macrophages. (4) Amastigotes multiply by simple division and infect other macrophages. (5), (6) Sand fly infects by taking a blood meal and ingesting parasitized cells. (7) In the midgut of the sand fly, amastigotes transform into promastigotes. (8) Promastigotes divide in the gut and migrate to the proboscis. Adapted from https://www.cdc.gov/dpdx/leishmaniasis/index.html. Created with BioRender.com.*

1.2 Macrophages as host cells for *Leishmania*

Macrophages serve as the major host cells for *Leishmania* in mammals (Goto et al. 2023). Because of this, the immune cells play a crucial role in the pathology of leishmaniasis, deciding the severity of the infection by enhancing or diminishing parasite growth (Goto and Mizobuchi 2023). Interestingly, *Leishmania* initially inhabit neutrophil granulocytes, but the promastigotes cannot transform inside the neutrophils, which is why they infect macrophages, where penetration and differentiation are possible (Podinovskaia and Descoteaux 2015).

However, there are different challenges that the parasites need to defeat in order to survive within the host (Goto et al. 2023).

In general, macrophages recognize pathogens by pathogen-associated molecular patterns and pattern-recognition receptors, normally resulting in phagocytosis, inflammation or other defense mechanisms (Lee and Bensinger 2022). During the prime interaction between the parasites and the host cells, *Leishmania* are in their promastigote form. Different studies imply

that there must be recognition or binding sites at the macrophage membrane to ease attachment since the promastigotes are not able to enter the macrophages on their own. Once the promastigotes have entered the macrophages, they can hide within the phagolysosome and continue their transformation (Pearson et al. 1983).
Due to the isolation from the macrophage cytosol and extracellular fluid, the parasite's nourishment, like the iron intake, is limited, requiring special molecules to enable nutrition and maintain survival (Goto et al. 2023).

To prevent the parasite from spreading, the macrophages have employed various defense mechanisms. These involve the formation of NADPH oxidase and inflammasomes complex in order to generate reactive oxygen species (ROS) to combat *Leishmania*. However, the parasite avoids host immune responses by inhibiting ROS production, inducing autophagy or affecting antigen presentation (Podinovskaia and Descoteaux 2015).

1.3 Model systems

To assess potential antileishmanial drugs in the research of new therapies, performing *in vitro* and *in vivo* tests is necessary. In general, *Leishmania* can be cultivated *in vitro* as promastigotes and amastigotes in axenic conditions. *In vitro* testing offers quick and reproducible results, enabling the examination of a broad range of drugs. Nevertheless, for compounds that express their activity through metabolites or the host immune system, *in vivo* testing is needed (Gupta and Nishi 2011).

Different species of *Leishmania* can be used for experiments. One example are *Leishmania tarentolae* promastigotes (LtP) which are derived from the gecko *Tarentolae annularis* (Cao et al. 2019). An essential benefit of LtP is their ability to be cultivated and maintained in normal laboratories since they are classified as biosafety class 1 organisms in contrast to most other *Leishmania* species classified in biosafety class 2 or even 3 (Taylor et al. 2010, Varotto-Boccazzi et al. 2021). In addition, the promastigotes grow in a continuous culture under aerobic conditions at 26 °C. Another advantage is the possibility of expanding to large-scale production (Mendoza-Roldan et al. 2022).
Furthermore, LtP can transform into amastigotes and infect macrophages *in vitro* (Cao et al. 2019). Their immunological resemblance to pathogenic *Leishmania* species makes them a potential target for antigen production and vaccine development (Bandi et al. 2023). Moreover, LtP are non-pathogenic in humans and mice, making them an efficient and safe model system

in the research for novel antileishmanial drugs (Cao et al. 2019).

Additionally, an adequate host cell model is crucial for testing different compounds. Hence, various studies on leishmaniasis have been performed over the years, involving experiments with inbred mouse strains like BALB/c and C57BL/6 mice (Goto and Mizobuchi 2023). Another instance are J774 mouse macrophages derived from bone marrow, used in testing the sensitivity of antileishmanial compounds (Bolhassani et al. 2011). In a previous study, J774 macrophages and LtP were used for testing the selectivity as well as comparing the antileishmanial activity of certain compounds for both cell cultures (Machin et al. 2022).

1.4 Sterols in *Leishmania* and macrophages

One essential biological distinction between *Leishmania* and mammalian cells is the sterol composition of their membranes (McCall et al. 2015).
In protozoans, lipids are known to influence energy production, membrane organization along with host-parasite interactions (Karamysheva et al. 2021). Endpoints of sterol metabolism in *Leishmania* parasites are ergosterol and ergosterol-like sterols (Fig. 2) (McCall et al. 2015). However, the most abundant sterols in *Leishmania* are considered to be 5-dehydroepisterol (5-DHE) and episterol (Torres-Santos et al. 2009).
Due to their specific lipid composition and fatty acid profile, *Leishmania* have a great chance of evading host immune responses, making the sterol biosynthesis pathway a potential target for the development of novel therapies (Mathur et al. 2015).

In mammals, there are many different sterols, but the most prevalent lipid with 30 % of the total lipids is the hydrophobic cholesterol (Chol) (Lee and Bensinger 2022). Chol (Fig. 2) plays an essential role in macrophages as it influences signal transduction and gene regulation (Yan and Horng 2020). Another sterol is 7-dehydrocholesterol (DHChol) which acts as a precursor of cholesterol in mammals (Fig. 2) (Xu et al. 2010).

Moreover, it was proven that the lipid metabolism adapts to host defense activity (Lee and Bensinger 2022). Hence, activating macrophages, phagocytosis or inflammatory cytokine production are lipid-dependent processes (Yan and Horng 2020). It has been shown that a certain cholesterol content in macrophages is required for *Leishmania* to infect these host cells (Pucadyil et al. 2004).

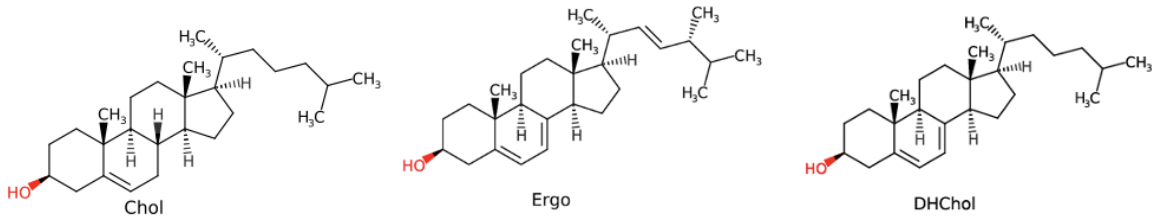

Figure 2: *Structure of cholesterol (Chol), ergosterol (Ergo) and 7-dehydrocholesterol (DHChol). The corresponding hydroxyl groups are highlighted in red.*

1.5 Antileishmanial drugs

The first approach for the treatment of any type of leishmaniasis were for a long time pentavalent antimony compounds (Alven and Aderibigbe 2020). Antimonials are prodrugs, meaning they need to be converted to their trivalent form in order to show activity against *Leishmania*. They work by inhibiting DNA topoisomerase 1 and interfering with the glutathione of trypanosomatids (Singh et al. 2023). Nevertheless, patients treated with antimonials suffer severe side effects (Alven and Aderibigbe 2020). For infected patients who are not susceptible to antimony compounds, pentamidine is used as a substitute (Singh et al. 2023).

The antimycotic drug amphotericin B is active against visceral leishmaniasis through autooxidation and binding to sterols in the membrane of the parasite (Taslimi et al. 2018). With the lipids bonded the cell membrane loses its stability, ultimately leading to cell death (Elawad et al. 2023). Amphotericin B is also used for patients with coinfections of HIV and pregnant women (Singh et al. 2023). Especially, the liposomal encapsulated formulation of amphotericin B, known as AmBisome (50 mg infusion for 120 min, i.v., AmBisome®, Gilead Sciences Inc., San Dimas, USA), has proven useful since it showed reduced innate kidney toxicity compared to other formulations of amphotericin B (Alpizar-Sosa et al. 2022). However, amphotericin B is rather expensive and normally applied intravenously, limiting its application to hospitals (Feng et al. 2022, Alven and Aderibigbe 2020).

Another antileishmanial drug is miltefosine, which acts as an anticancer and antileishmanial drug against the visceral and cutaneous forms. Even though miltefosine is beneficial due to its oral intake, its teratogenic properties are increased due to its long half-life (Taslimi et al. 2018). Therefore, the drug is not registered for treating pregnant women. Notably, miltefosine did not

demonstrate antileishmanial activity in studies with BALB/c mice infected with *L. braziliensis* and *L. amazonensis*, implying limitations for these species of *Leishmania* (Singh et al. 2023).

Interestingly, the majority of antileishmanial compounds was repurposed. For instance, azoles are mainly used against yeasts and molds. They work by causing stress on the cell membrane through blocking the oxygen required for demethylation of lanosterol 14-α-demethylase, the major enzyme in sterol synthesis in yeasts. In *Leishmania,* azoles target the synthesis of the main sterols of the cell membrane, ergosterol-like sterols (Braga 2019). Azoles such as fluconazole, ketoconazole and itraconazole can be taken orally (Alven and Aderibigbe 2020). There are also other compounds like miltefosine that impact the lipid metabolism (Karamysheva et al. 2021).

Increasing drug resistance and toxicity of compounds pose serious problems for the treatment of leishmaniasis (Alven and Aderibigbe 2020). Therefore, research for new, effective and affordable drugs is necessary (Mendes et al. 2022).

1.6 Endoperoxides

Organic endoperoxides widely exist in organisms as metabolic intermediates or secondary metabolites. Well-known intermediates in prostanoid synthesis in mammals are PGG_2 and PGH_2. The cyclooxygenase transforms the arachidonic acid into the prostaglandin endoperoxide, PGG_2 (Plastaras et al. 2000). Many plants produce endoperoxides (EPs) as a defense against microorganisms.

EPs are known to be effective against bacteria, fungi and protozoa, including parasites like *Trypanosoma cruzi* (Merdivan and Lindequist 2017). Moreover, endoperoxides exhibit anticancer activity in colorectal cancer, hepatocellular carcinoma or leukemia, for instance (He et al. 2018). EPs all share cyclic peroxide structures and are widely spread in nature (Mori and Abe 2022). The characteristic feature in the structure of organic peroxides is the peroxide group (O-O), which connects to two different carbon atoms of the same molecule, forming a ring structure (Merdivan and Lindequist 2017). EPs are known for their rapid reaction with biologically relevant transition metals, such as Fe^{2+} and Cu^{+}, as explained later (O'Neill and Posner 2004).

Due to the natural occurrence of EPs in plants or other organisms, they can be isolated in high-performance liquid chromatography or similar column chromatography (He et al. 2018).

1.6.1 Ergosterol endoperoxide

Ergosterol endoperoxide (ErgoEP), derived from a lipid-soluble C28-sterol, exhibits antimicrobial, cytotoxic and immunosuppressive activities (Fig. 3) (Merdivan and Lindequist 2017). It is found in mushrooms, plants or lichens and is derived from the photosensitized oxidation of ergosterol (Tian et al. 2017). In addition, ErgoEP has exhibited activities against cancer and viruses (Mori and Abe 2022).

1.6.2 Dehydrocholesterol endoperoxide

DHChol (Fig. 2), the biosynthetic precursor of cholesterol and vitamin D3, is an analogue of ergosterol in mammals (Tian et al. 2017). It is found in the skin of animals since it is a derivate of cholesterol (Wang et al. 2019). After UV irradiation, DHChol is converted to vitamin D3 in human and mammalian skin (Tian et al. 2017). It can be transformed into DHChol endoperoxide (DHCholEP) (Fig. 3) in chemical synthesis through photo-oxidation via singlet oxygen (Wang et al. 2019).

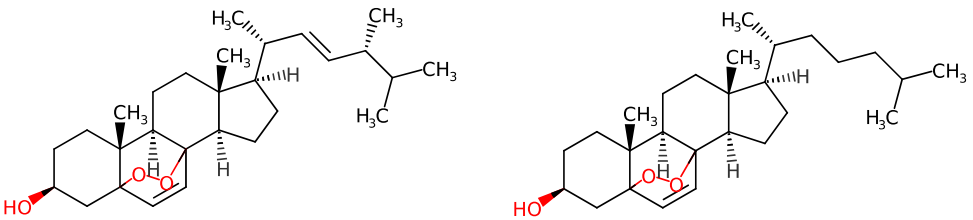

Figure 3: *Structure of ergosterol endoperoxide (ErgoEP) and dehydrocholesterol endoperoxide (DHCholEP). The corresponding peroxide and hydroxyl groups are highlighted in red.*

1.7 Possible targets in *Leishmania*

Uptake of promastigotes in host neutrophils and macrophages under survival of the parasites in the phagolysosome and subsequent transformation to amastigotes, as well as their further survival and proliferation, represent an extreme adaptation of the parasites to their host cell environment (Kaye and Scott 2011). Besides the passive adaptation of parasites, they developed methods to influence host cell signaling and metabolism to ensure their intracellular survival. In the cell culture of LtP but also for intracellular amastigotes in host cells, iron is an essential nutritional factor, which amastigotes acquire in the form of low molecular iron and heme through several transporters from the host cell, influencing host cell iron metabolism

(Kaye and Scott 2011). This results in leishmania possessing a rather large intracellular labile iron pool (more than macrophages), which makes them highly susceptible to peroxides (including organic endoperoxides) (Marquis and Gros 2007, Flannery et al. 2013, Laranjeira-Silva et al. 2020).

Due to this fact, endoperoxides have been explored as antileishmanial agents (Geroldinger et al. 2018).

Antiparasitic activity against different protozoans, such as *L. infantum,* was observed for the sesquiterpene lactone endoperoxide artemisinin, for example, and other synthetic endoperoxides like trioxanes, trioxolanes or tetraoxanes (Mendes et al. 2022).

Artemisinin is derived from *artemisia annua,* an ancient Chinese herbal remedy also known as sweet wormwood. Chinese herbal medicine practitioners have been using this plant for centuries (Meshnick 2002). In general, the endoperoxide artemisinin is known for its activity against malaria (Tian et al. 2017). Hereby, the peroxidic core of artemisinin has an essential role for the modes of bioactivation and action against the parasites. The release of heme (Fe^{2+}) during parasite hemoglobin digestion reductively activates the peroxide (O-O) bond. This leads to the separation of the endoperoxide ring, causing the formation of ROS and the promotion of cell death (Mendes et al. 2022).

Another natural peroxide from the essential oil of *Chenopodium ambrosioides* is ascaridole (Pastor et al. 2015).

Previous studies in LtP demonstrated that artemisinin in contrast to ascaridole increasingly interacted with heme instead of low molecular iron in LtP. Furthermore, synthetic anthracene endoperoxides were also effective against LtP, while antileishmanial activity and selectivity for LtP over J774 cells depended on their structure (Machin et al. 2022).

These observations demonstrate that the residual structure has a significant influence on the antileishmanial activity and selectivity. This indicates that pharmacological mechanisms beyond the endoperoxide group and radical formation have to be taken into account, implying additional specific targets.

For example, for ErgoEP, antiparasitic activities were observed against Chagas disease (Merdivan and Lindequist 2017). It was also demonstrated that the compound can activate Foxo3-mediated cell death in cancer cells (Li et al. 2016). However, whether there are additional mechanisms of action beyond radical formation was rarely addressed.

Therefore, the actual targets of sterol EP in Leishmania are still unknown.

1.8 Aims of the work

The focal point of this bachelor thesis was testing sterol EPs (ErgoEP and DHCholEP) impact on LtP and J774 macrophages as models for pathogenic *Leishmania* and for host macrophages.

Therefore, the performed experiments aimed to assess:

(i) the influence of ErgoEP and DHCholEP on the viability of LtP and J774 macrophages.

(ii) the interference of antioxidants (N-acetyl cysteine (NAC), butylated hydroxytoluene (BHT) and 6-hydroxy-2,5,7,8-tetramethylchroman-2-carboxylic acid (Trolox)) in the antileishmanial effects of sterol EP and reference compounds on the viability of LtP.

(iii) the impact of ErgoEP and DHCholEP on sterol synthesis in LtP.

(iv) the suitability of an extraction standard for improvement of sterol quantitation, counteracting methodological limitations and increasing reproducibility in regard to prospective experiments.

2. Materials and methods

2.1 Chemicals

The chemicals listed in Table 1 were used for sample preparation and maintenance.

Table 1: *Chemicals used for sample preparation and maintenance.*

Chemical	Supplier
6-Hydroxy-2,5,7,8-tetramethylchroman-2-carboxylic acid (Trolox)	Sigma-Aldrich (St. Louis, Missouri, USA)
7-Dehydrocholesterol (DHChol)	Sigma-Aldrich (St. Louis, Missouri, USA)
Acetonitrile (ACN)	Merck (Darmstadt, Germany)
Amphotericin B (AmpB)	Cayman Chemical
Antimycin A (AA)	Sigma-Aldrich (St. Louis, Missouri, USA)
Artemisinin (Art)	Sigma-Aldrich (St. Louis, Missouri, USA)
Brain heart infusion medium (BHI)	Sigma-Aldrich (St. Louis, Missouri, USA)
Butylated hydroxytoluene (BHT)	Roche (Basel, Switzerland)
Corticosterone (CCS)	Sigma-Aldrich (St. Louis, Missouri, USA)
Dehydrocholesterol endoperoxide (DHCholEP)	Self-synthesized
Dimethyl sulfoxide (DMSO)	VWR (Radnor, Pennsylvania, USA)
Dulbecco's modified eagle's medium (DMEM)	Thermo Fisher Scientific (Waltham, MA, USA)
Ergosterol (Ergo)	Acros Organics (Geel, Belgium)
Ergosterol endoperoxide (ErgoEP)	Self-synthesized
Ethanol (EtOH)	Scharlab (Barcelona, Spain)
Fetal calf serum (FCS)	Bio & Sell (Nuremberg, Germany)
Hemin	Sigma-Aldrich (St. Louis, Missouri, USA)
Itraconazole (ItraAz)	Thermo Fisher Scientific (Waltham, MA, USA)
KCl	Merck (Darmstadt, Germany)
K_2HPO_4	Merck (Darmstadt, Germany)
Ketoconazole (KetoAz)	Thermo Fisher Scientific (Waltham, MA, USA)
KH_2PO_4	Merck (Darmstadt, Germany)
Methanol (MeOH)	Merck (Darmstadt, Germany)
Miconazole (MiAz)	Thermo Fisher Scientific (Waltham, MA, USA)
Miltefosine (Mil)	Thermo Fisher Scientific (Waltham, MA, USA)
N-acetyl cysteine (NAC)	Thermo Fisher Scientific (Waltham, MA, USA)
n-Hexane (Hx)	Merck (Darmstadt, Germany)
Na_2HPO_4	Merck (Darmstadt, Germany)
NaCl	Merck (Darmstadt, Germany)
Penicillin-streptomycin solution	VWR (Radnor, Pennsylvania, USA)
Pentamidine (Pen)	Sigma-Aldrich (St. Louis, Missouri, USA)
Potassium hydroxide (KOH)	Merck (Darmstadt, Germany)
Resazurin	Sigma-Aldrich (St. Louis, Missouri, USA)
Yeast extract (YE)	Amresco (Solon, Ohio, USA)

2.1.1 Structures of compounds

The chemical structures of the control compounds are shown below in Figure 4.

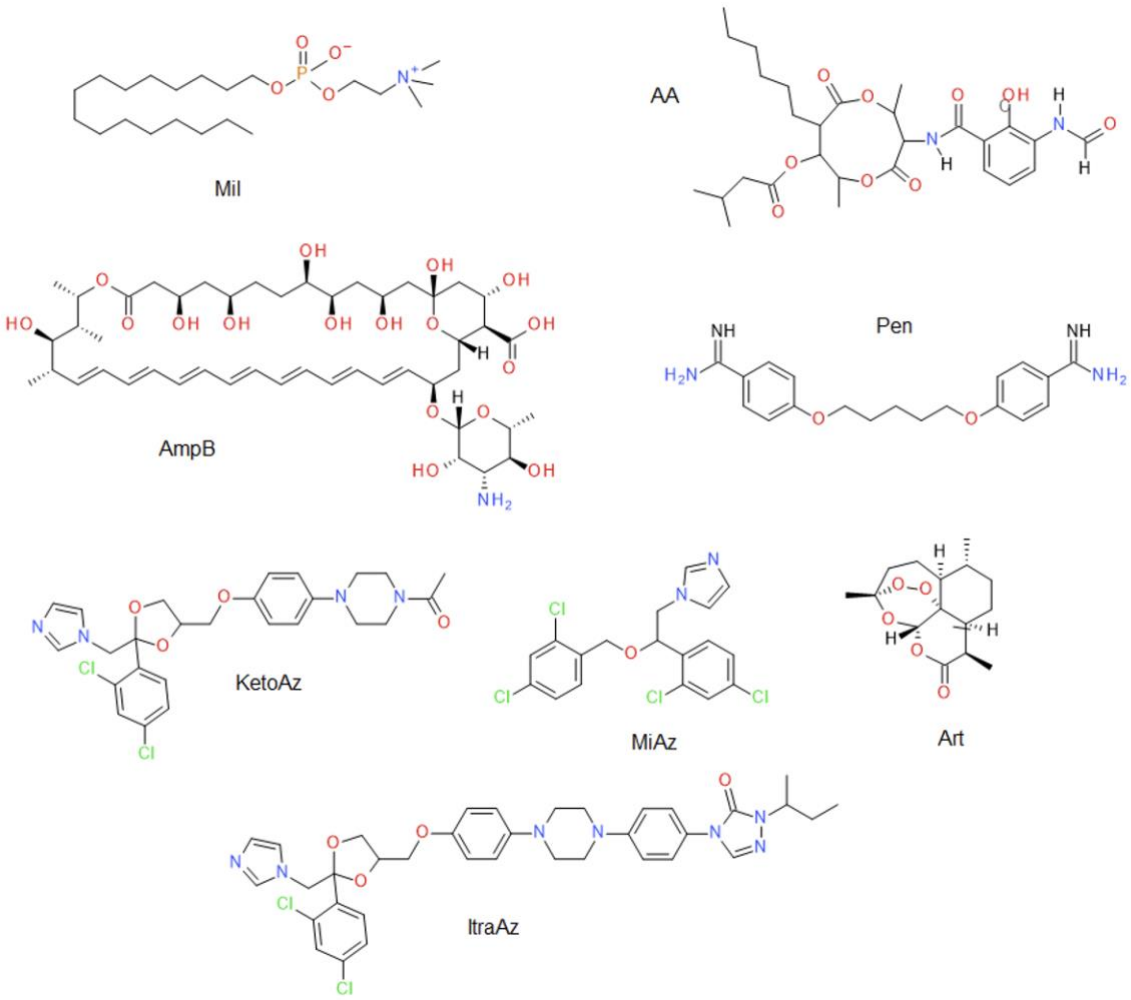

Figure 4: *Chemical structures of miltefosine (Mil), antimycin A (AA), amphotericin B (AmpB), pentamidine (Pen), ketoconazole (KetoAz), miconazole (MiAz), itraconazole (ItraAz) and artemisinin (Art).*

2.1.2 Stock solutions

Stock solutions were prepared in ACN (AA), DMSO (Pen, Mil, AmpB, ItraAz, Art) or EtOH (Ergo, ErgoEP, DHChol, DHCholEP, KetoAZ, MiAZ, NAC, BHT, Trolox).
Solutions of Ergo and DHChol were produced every 3–4 weeks to limit possible degradation.

2.2 LtP cell culture

One part of the experiments for this thesis was carried out with LtP as a model system (strain

P10, Jena Bioscience, Germany). For the cultivation of the cells, BHI medium (37 g/L, pH 7.4) was supplemented with 5 mg/L hemin, 25000 IU/L penicillin and 25 mg/L streptomycin. LtP were cultivated in 50 mL TubeSpin bioreactors and 10–15 mL culture per tube was incubated at 26 °C (Cytoperm, Heraeus Instruments, Hanau, Germany).

The cells were counted using a photometer (U-1100, Hitachi Ltd, Tokyo, Japan) and measuring the OD at 600 nm. The cell concentration was then calculated with the following formula:

$$OD_{600} * 0.969 * 124 * 10^6 = \frac{LtP}{mL}$$

0.969: $conversion\ factor\ wet\ \left(\frac{g}{L}\right) - dry\ weight\ (g)$

124: $1\ g\ dry\ weight/L = 124 \times 10^6\ LtP/mL$

The passage of the cells took place on Mondays, Wednesdays and Fridays. The target OD of the cells was 0.3 on Mondays and Wednesdays and 0.15 on Fridays, expecting a respective cell density of 36 * 10^6 LtP/mL and 18 * 10^6 LtP/mL.

2.3 J774 cell culture

The other part of the experiments involved a murine macrophage cell line, J774A.1 (mouse, ATCC, TIB-67™). The cultivation of the J774 cells was performed in 50 mL TubeSpin bioreactors or 25 cm² rectangular canted neck cell culture flask with vented caps (Falcon®) with DMEM (high glucose, 1.5 g/L $NaHCO_3$), 25,000 IU/L penicillin, 25 mg/L streptomycin and 10 % heat-inactivated FCS. The incubation of the macrophages (10 mL in TubeSpin bioreactors, 6 mL in cell culture flasks) took place at 37 °C on a roller culture apparatus (5 rpm) (TubeSpin bioreactors) or stationary (cell culture flasks) with 5 % CO_2. The cell culture was passaged two times a week, on Tuesdays to a density of 0.2 * 10^6 cells/mL and on Fridays to a density of 0.1 * 10^6 cells/mL. In stationary cell culture flasks, the cells were removed by a scraper and then suspended in medium for counting and passage, while in bioreactors the cells were maintained in suspension. For the cell count, an aliquot of the cell suspension was applied to a Thoma chamber, and 8 pictures were taken of each chamber with the integrated camera of the microscope. Afterwards, the pictures of the cells were analyzed with a customized cell image analysis (CIA, own design) software.

2.4 Viability assays

2.4.1 LtP

For this thesis, the viability assays for LtP were all conducted in 96-well uncoated culture plates (Eppendorf, Art. nr. 30730011). Two distinct viability assays with LtP were performed, one with horizontal concentration gradients and the other one with vertical concentration gradients. For the horizontal assay, three compounds were tested in duplicate at twelve different concentrations. In the vertical combination assay, two substances at six different concentrations were tested in triplicate in the presence or absence of a radical scavenger.

Before carrying out the viability assays for LtP, a mixture of yeast extract medium (YEM) (20.7 g/L yeast extract powder, 1.2 g/L K_2HPO_4, 0.2 g/L KH_2PO_4, 2.9 g/L glucose monohydrate, pH 7.4) and PBS (136 mM NaCl, 1.15 mM KH_2PO_4, 14 mM Na_2HPO_4, and 2.7 mM KCl, pH 7.4) was prepared in a 1:1 ratio. 25,000 U/L penicillin, 25 mg/L streptomycin, and 6 µM hemin were added to the mixture, which was then used as the assay medium. On the day of testing, which was one day after the LtP passage, one part of the YEM/PBS medium was enriched with $2 * 10^6$ LtP/mL, later used as a cell suspension in the assay.

For the horizontal viability assays demonstrated in Figure 5, 200 µL of YEM/PBS was applied as a negative control in row A in columns 1–6 and row H in columns 7–12. Then 100 µL YEM/PBS was added to the test wells in rows B–G, row A in columns 7–12 and row H in columns 1–6. In the following step, additional YEM/PBS medium was applied in column 1 B–G as well as the aliquots of compound stocks, giving the respective maximal concentration for each individual compound in the 200 µL total volume. Afterwards, a 1:2 serial dilution (transferring 100 µL) was performed from columns 1–12 in rows B–G, except for KetoAz, MiAz and ItraAz a 1:5 serial dilution was conducted (transferring 25 µL, 125 µL total volume before dilution). 100 µL of the above-mentioned cell suspension was finally added to the test wells (B–G) and to the positive control wells (cells only, row A, 7–12; row H, 1–6). In the last step, the gaps between the wells were filled with 8 mL of PBS for humidity control, and the plates were incubated for 48 h at 26 °C.

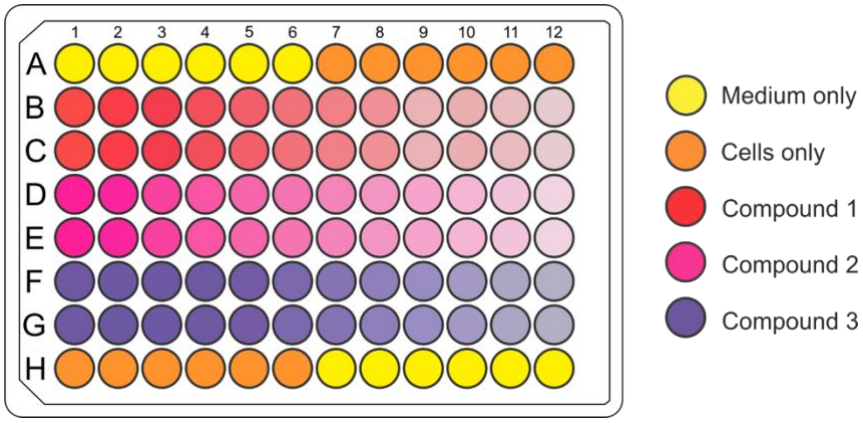

Figure 5: *Graphic representation of the horizontal viability assay. Row A (1–6) and row H (7–12) containing only YEM/PBS, were used as a negative control, while row A (7–12) and row H (1–6) only contained YEM/PBS with cell suspension, serving as a positive control (cells only). The compounds, three on each plate, and cell suspension with YEM/PBS were applied in column 1 from row B to G in duplicate. A 1:2 serial dilution was performed from column 1 (highest concentration) to column 12 (lowest concentration) in rows B–G.*

For the vertical combination viability assays shown in Figure 6, the first step was adding the radical scavengers NAC or BHT or Trolox in different concentrations (2 mM NAC, 10 µM BHT, 200 µM Trolox) to one part of the cell suspension. The other part of the cell suspension remained the same. Afterwards, the wells were filled with 200 µL YEM/PBS (negative control wells) in row A and with 200 µL control cell suspension in columns 1–6 in rows B–H (row B served as a positive control with only cells). Furthermore, 200 µL of the cell suspension treated with the radical scavenger was applied in columns 7–12 in rows B–H, along with the extra control cell suspension with and without the radical scavengers in row H, respectively. Then the aliquots of the compound stocks were distributed in row H giving 300 µL total volume and a 1:3 serial dilution (transferring 100 µL) was performed from row H to C. Lastly, 8 mL PBS was placed between the wells, and the plates were incubated for 48 h at 26 °C.

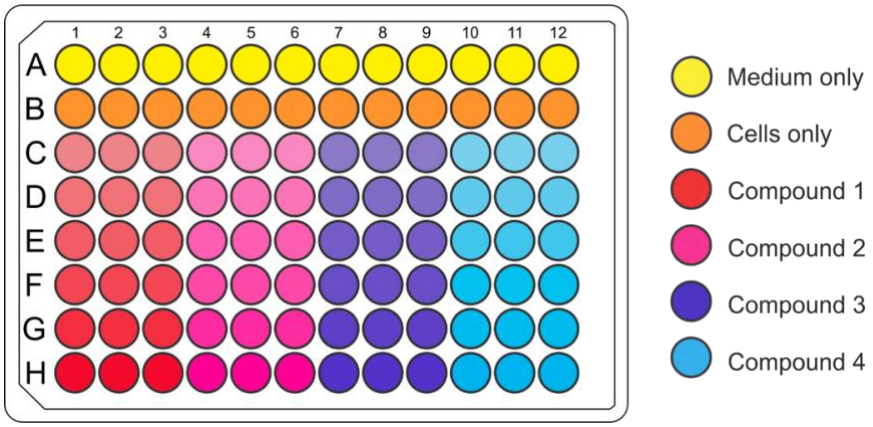

Figure 6: *Graphic representation of the vertical combination viability assay. Row A was used as a negative control only containing YEM/PBS, while row B served as a positive control containing only cells. Compound 1 and compound 2 were not treated with a radical scavenger (N-acetyl cysteine, butylated hydroxytoluene or 6-hydroxy-2,5,7,8-tetramethylchroman-2-carboxylic acid), contrary to compounds 3 and 4. Rows C–H contained YEM/PBS with cell suspension and compounds in triplicate. A 1:3 serial dilution was performed from row H to C (highest to lowest concentration).*

After the incubation, 50 µL of resazurin as a viability indicator was added to each well for both types of assays, giving a final concentration of 20 µM. Subsequent to another incubation of 4 h at 26 °C, the fluorescence of the plates was measured with a plate reader (Varioskan, Thermo Fisher Scientific, Waltham, USA) at 560 nm excitation and 590 nm emission. To calculate the viability (%) of each well, the fluorescence values of the wells with YEM/PBS medium (F_{medium}), the wells with the corresponding compounds (F_{comp}) and the wells only containing cells (F_{cells}) were considered, and the following equation was used:

$$Viability\ (\%) = \frac{F_{comp} - F_{medium}}{(F_{cells} - F_{medium})}$$

2.4.2 J774

For the J774 macrophages, horizontal viability assays were conducted in 96-well TC-treated plates (Eppendorf, Art. nr. 30730119), according to the scheme in Figure 5. A cell suspension was prepared, containing DMEM, 25,000 U/L penicillin, 25 mg/L streptomycin, and 10 % FCS, along with 0.2 * 10^6 J774/ml per well. The first step was adding 200 µL DMEM as a negative control to row A in columns 1–6 and row H in columns 7–12, and 100 µL DMEM to the test wells (B–G), row A in columns 7–12 as well as row H in columns 1–6 (positive control). Moreover, the wells in column 1 (B–G) were filled with additional medium and aliquots of the

compound stocks in corresponding concentrations (giving 200 µL of total volume). Subsequent to the 1:2 serial dilution (transferring 100 µL), 100 µL of the cell suspension was distributed to the test wells (B–G), row A in columns 7–12 and row H in columns 1–6. Furthermore, 8 mL of PBS was placed between the wells, and the plates were incubated for 48 h at 37 °C and 5 % CO_2. After the incubation, 50 µL of resazurin was added to the wells, giving a final concentration of 20 µM. After 4 h at 37 °C, the fluorescence was measured at 560 nm excitation and 590 nm emission using a plate reader (Varioskan, Thermo Fisher Scientific, Waltham, USA). The viability was calculated in the same way as for LtP.

2.5 Batch incubation with sterol EP

At first, 45 mL of BHI medium was distributed to each 50 mL blue cap Falcon tube as well as an aliquot of the ongoing LtP cell culture, typically one day after the passage, targeting an optical density of 0.3 at 600 nm. After the OD measurement of the cell suspension, the corresponding concentrations of the compounds (ErgoEP and DHCholEP) or the vehicle control (EtOH) were included. Then, 15 mL of the cell suspension containing the compounds or vehicle was distributed into 50 mL blue cap Falcon tubes with holes for aeration. The samples were prepared in triplicate for each concentration. The cells were incubated for 24 h, and the cell density was measured photometrically after 0, 6 and 24 h. The percentage of LtP viability was calculated before the sterol extraction using the cell density measured after 24 h.

2.5.1 Sterol extraction

Prior to the extraction process, 25 mL of the saponification solution (6.25 g KOH, 8.75 mL H_2O in EtOH) was prepared, and empty 5 mL Eppendorf (EDF) tubes were weighed. Then, the OD of the cells was measured after 24 h at 600 nm and the LtP were spun down in 50 ml Tubes (3000 x g, 10 min, 20 °C). Afterwards, the supernatant was removed, the pellets were resuspended in 5 mL PBS and transferred to the EDF tubes. After the centrifugation of the PBS suspension (4000 x g, 10 min, 20 °C), the supernatant was removed and the LtP pellet mass was weighed for each EDF tube. In the next step, 1.5 ml of the prepared saponification solution was distributed to each tube. Then, the tubes were incubated for 1 h at 85 °C and vortexed every 15 min. Once the tubes had cooled down to room temperature, 0.5 mL of H_2O and 1.5 ml of n-hexane were added to each tube. After mixing on an Eppendorf thermomixer (900 rpm, 30 min, 20 °C) and subsequent centrifugation (4000 x g, 10 min, 20 °C), the organic phase (1.2 mL) was transferred to an empty 1.5 mL tube. The organic layer in the EDF tubes was evaporated under a stream of N_2, the dried extracts were dissolved in ACN (1.2 mL), and

then, transferred to high-performance liquid chromatography (HPLC) vials (Fig. 7).

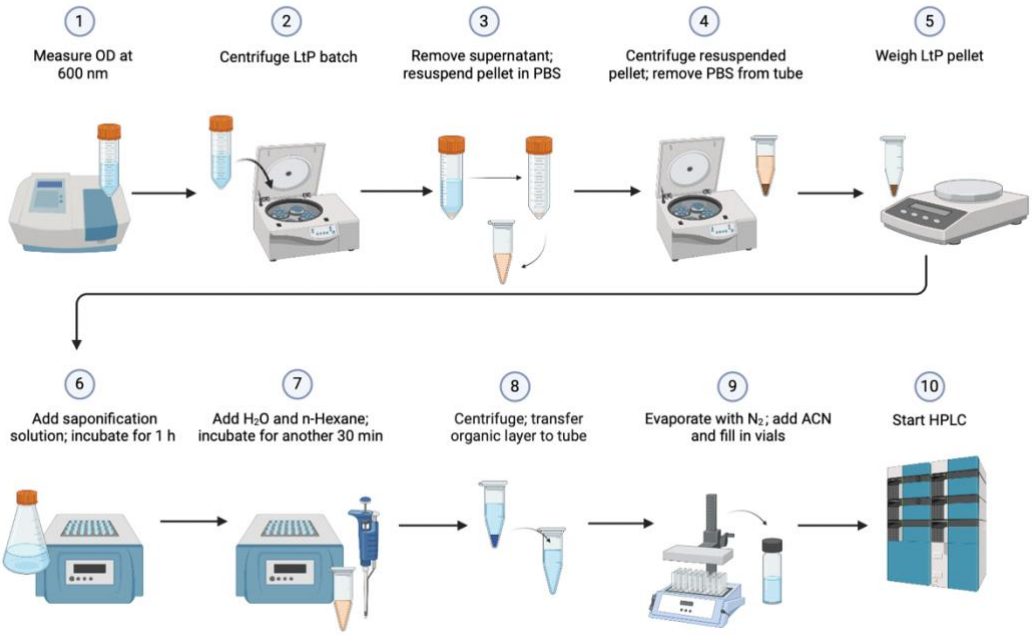

Figure 7: *Schematic representation of the sterol extraction procedure for LtP batches for high-performance liquid chromatography (HPLC). Created with BioRender.com.*

2.6 High-performance liquid chromatography

The HPLC analysis was conducted in a Shimadzu LC-20 system with an included dual-wavelength UV detector and the LCSolutions software. A volume of 10 µL of each sample was injected by the integrated autosampler on an RP-8 column (LiChrospher®, analytical grade RP-8, particle size 5 µm, ID 4 mm, length 250 mm) with a pre-column (LiChrospher®, RP-8, particle size 5 µm, ID 4 mm, length 4 mm). Samples were eluted with 10 % H_2O and 90 % of a solvent mixture (ACN:MeOH, 99:1) for 45 min and detection was performed in a 205 nm and a 281 nm channel. For quantification, the areas of the peaks of interest were measured using the LCSolutions software.

2.6.1 LtP batches with internal standard

To further improve quantitation and counteract losses during liquid-liquid extraction, CCS was employed as a potential internal standard. The first step was to determine the UV spectrum (200 nm to 370 nm) of CCS (100 µM in EtOH, using EtOH as a reference). Subsequently, CCS (500 µM CCS in ACN) was analyzed in HPLC at 205 nm, 241 nm (only the first 5 min) and 281 nm.

To study CCS as a possible internal standard in LtP batches, an aliquot of the compound was mixed with n-hexane to achieve a 250 µM CCS solution. The n-hexane containing CCS was then applied to the samples prior to the second incubation, followed by completing the remaining steps as described above (Fig. 7).

2.7 Data treatment and statistics

The data analysis and the graphs were executed in Excel (Microsoft). The IC_{50} values were calculated from viability (Viab)-concentration (Conc) curves with an Excel worksheet including python applications using a four-parameter logistic model (Hill-Slope model) (Müllebner et al. 2009) according to the following formula:

$$Viab = I_{bot}\ \frac{(I_{top} - I_{bot})}{(1 + (\frac{Conc}{IC_{50}})^{Slope}}$$

In this work, a model with a fixed I_{top} and I_{bottom} (0 % viab) was used and I_{top} was set to the maximum intensity.

IC_{50} values of replicates were averaged, and standard deviation was calculated. The number of replicates is given in the respective figures/tables.

3. Results

3.1 Influence of EP and related compounds on the viability of LtP and J774 cells

An informative *in vitro* measure for assessing the effectiveness of new antileishmanial drugs is the IC_{50} value, which determines the concentration at which the compounds exhibit 50 % inhibition of the viability of *Leishmania* and J774 cells. Typical examples of viability-concentration curves obtained from horizontal viability assays, performed for both LtP and J774 cells, are shown below (Fig. 8).

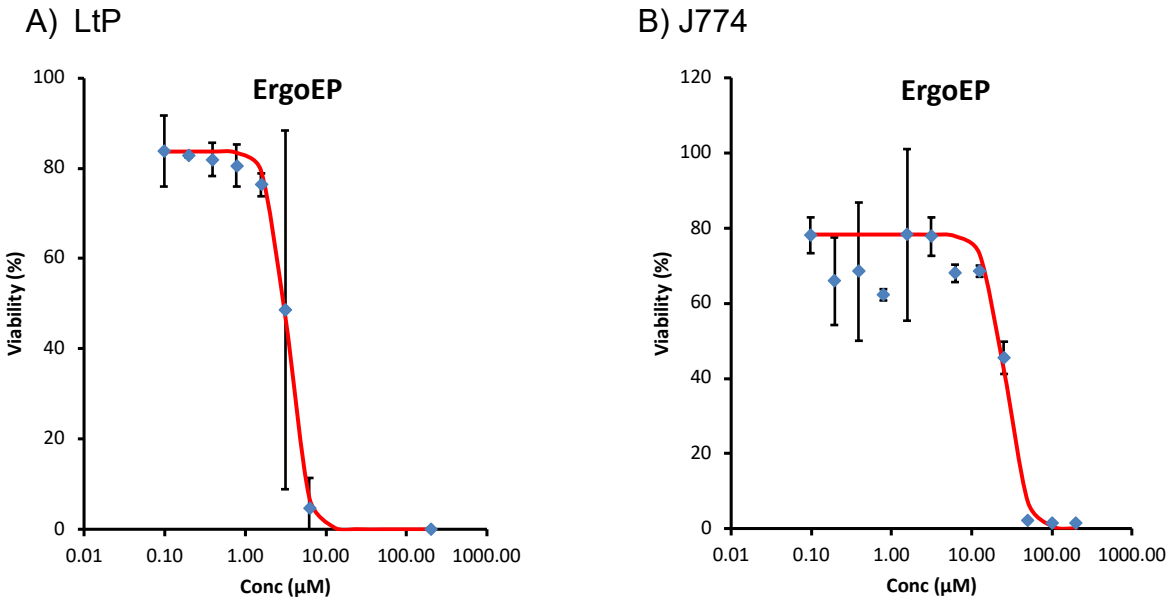

Figure 8: *Influence of ergosterol endoperoxide (ErgoEP) on the viability of LtP and J774 cells. Typical example of LtP (A) and J774 (B) viability (%) influenced by different concentrations (Conc; 0.098 µM–200 µM) of ErgoEP. Viability-concentration curves were established using a horizontal viability assay and calculating each data point by taking the mean ± standard deviation of wells (n = 2) from a single culture batch, resulting in IC_{50} values of 3.34 µM ± 0.10 for (A) and 26.23 µM ± 2.85 for (B).*

A comparison of the influence of ErgoEP on the viability of both cell types from a single culture batch shows that for LtP the viability decreased already at lower concentrations than for J774 (Fig. 8). Therefore, ErgoEP had a smaller IC_{50} value for LtP than for J774.

Moreover, for DHCholEP (Fig. 9) there is also a decrease in the viability of LtP at lower concentrations than for J774 cells and therefore, a lower IC_{50} value for LtP. Furthermore, the IC_{50} value for DHCholEP in LtP was lower than the corresponding value of ErgoEP.

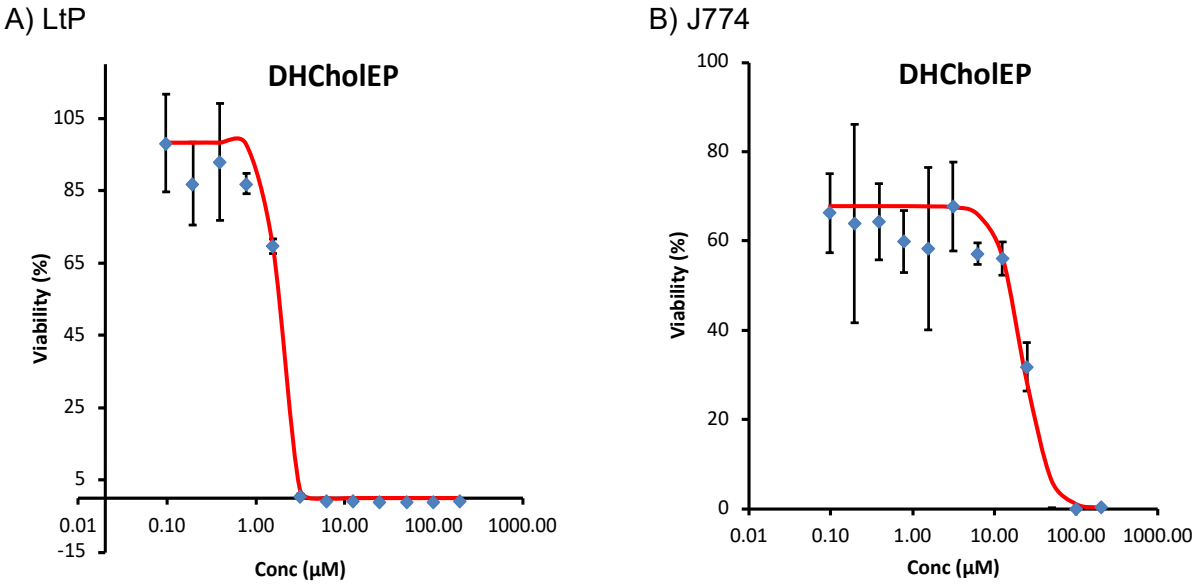

Figure 9: *Influence of dehydrocholesterol endoperoxide (DHCholEP) on the viability of LtP and J774 cells. Typical example of LtP (A) and J774 (B) viability (%) influenced by different concentrations (Conc; 0.098 µM–200 µM) of DHCholEP. Viability-concentration curves were established using a horizontal viability assay and calculating each data point by taking the mean ± standard deviation of wells (n = 2) from a single culture batch, resulting in IC_{50} values of 1.79 µM ± 0.13 for (A) and 22.22 µM ± 2.21 for (B).*

To evaluate the viability of both cell types in the presence of sterol EP and related compounds, viability assays were repeatedly (n = 5-7) performed and the respective IC_{50} values are summarized in Table 2.

To determine whether a substance is more selective towards LtP than J774, the IC_{50} values of J774 were divided by the IC_{50} values of LtP and thus, the selectivity factor was calculated.

Table 2: *Influence of sterol endoperoxides and related compounds on LtP and J774 viability. Comparison of mean IC_{50} value ± standard deviation (SD) of compounds for LtP and J774 (n = 5–7) and calculated selectivity factor for LtP over J774 ($J774\ IC_{50}$ / $LtP\ IC_{50}$). For LtP the concentrations of compounds ranged from 0.01 µM–20 µM for pentamidine (Pen), 0.098 µM–200 µM for ergosterol (Ergo), 0.098 µM–200 µM for ergosterol endoperoxide (ErgoEP), 0.098 µM–200 µM for 7-dehydrocholesterol (DHChol), 0.098 µM–200 µM for dehydrocholesterol endoperoxide (DHCholEP), 0.01 µM–40 µM for miltefosine (Mil), 0.001 µM–1.5 µM for amphotericin B (AmpB), 0.005 µM–10 µM for ketoconazole (KetoAz), 0.002 µM–5 µM for itraconazole (ItraAz), 0.01 µM–20 µM for miconazole (MiAz), 0.002 µM–5 µM for antimycin A (AA) and 0.024 µM–60 µM for artemisinin (Art). For J774, concentrations of Pen, Ergo, ErgoEP, DHChol and DHCholEP were in the same range as for LtP. Concentrations of the other compounds ranged from 0.01 µM–200 µM for Mil, 0.01 µM–100 µM for AmpB, 0.073 µM–200 µM for KetoAz, 0.068 µM–200 µM for ItraAz, 0.01 µM–20 µM for MiAz, 0.001 µM–40 µM for AA and 0.024 µM–60 µM for Art. For AA in J774 cells no total inhibition of viability was achieved, remaining at 50–60 % viability at 2 µM AA.*

Compound	**IC_{50} (µM) mean ± SD**		**Selectivity factor**
	LtP	**J774**	**(J774 IC_{50} / LtP IC_{50})**
Pen	0.790 ± 0.132	1.223 ± 0.795	2
Ergo	18 ± 14	22 ± 12	1
ErgoEP	4.5 ± 1.2	22 ± 5	5
DHChol	5.2 ± 4.7	17 ± 6	3
DHCholEP	2.0 ± 0.4	15 ± 5	8
Mil	0.267 ± 0.147	124 ± 43	464
AmpB	0.129 ± 0.034	32 ± 13	248
KetoAz	0.013 ± 0.020	17 ± 6	1307
ItraAz	0.042 ± 0.021	0.570 ± 0.389	14
MiAz	0.998 ± 0.199	26 ± 12	26
AA	1.755 ± 0.376	> 2 µM	–
Art	6.2 ± 1.1	17 ± 11	3

The results from Table 2 indicate IC_{50} values for sterol EPs in LtP in the low µM range being 5–8 times lower than the corresponding values in J774 cells. Mil, AmpB and KetoAZ had the highest selectivity factor in comparison to the other compounds.

3.1.1 Influence of sterols on LtP viability

Ergo and DHChol also demonstrated antileishmanial activities in these assays, although their IC_{50} values were always higher than the values of the corresponding sterol EPs. This effect is so far mechanistically unexplained. However, from previous work (Schrödl 2023) it is known

that Ergo and DHChol (triene sterols) showed antileishmanial activity in LtP in contrast to cholesterol at 200 µM (Chol, monoene sterol). It was demonstrated that Ergo and DHChol reacted with Fe^{2+} unlike Chol, suggesting some peroxide accumulation in stocks from Ergo and DHChol over time.

Therefore, the influence of Ergo stocks with different ages on the IC_{50} values in LtP was analyzed (Fig. 10).

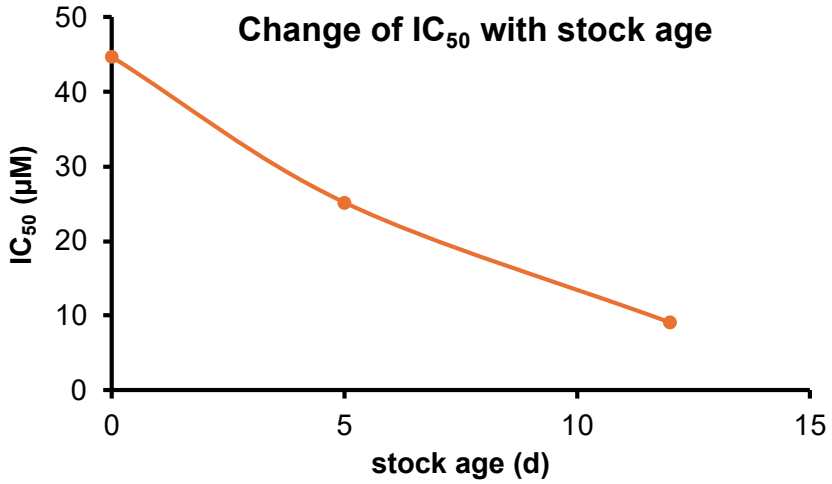

Figure 10: *Plot showing change of IC_{50} values of ergosterol (Ergo) for LtP in relation to the stock age (d). IC_{50} values were obtained in horizontal viability assays, measuring Ergo's influence on LtP viability. The stock age was set to zero for the first measurement.*

It was discovered that the IC_{50} values of Ergo stocks of different ages decreased over time, indicating an increase in their antileishmanial activity. The IC_{50} values were obtained from horizontal viability assays from distinct weeks, testing the influence of Ergo on LtP viability. The Ergo stocks received the same treatment process throughout the testing.

To investigate this effect further, HPLC analysis of Ergo stocks was performed, detecting retention times and peaks in the 205 nm and 281 nm channels (Fig. 11).

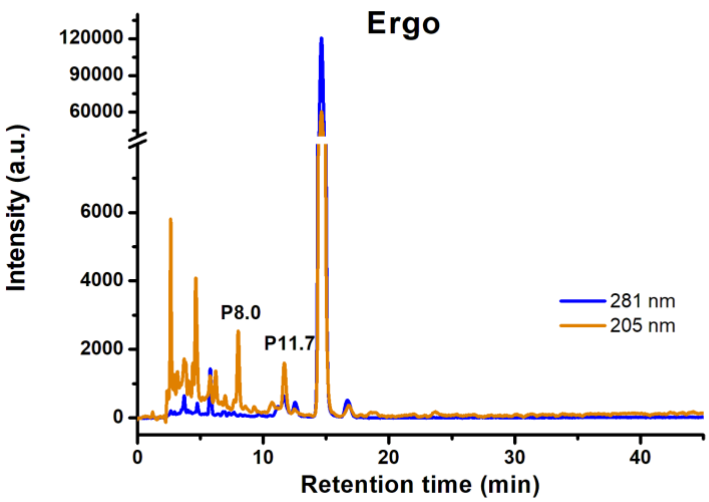

Figure 11: *Typical chromatogram of an ergosterol (Ergo) stock (prepared from commercial Ergo). 10 % H_2O/90 % solvent mixture (ACN:MeOH, 99:1) was used as eluent. The sample was prepared by adding 25 µL Ergo (20 mM) to 1000 µL acetonitrile. Retention times (min) of relevant peaks (P) recorded at 205 nm and 281 nm are shown.*

As expected, one major peak at 14.6 min (P14.6, > 95 % peak area in the 281 nm channel) was identified in both channels as well as minor peaks at 8.0 min (P8.0) and 11.7 min (P11.7) in the 205 nm channel, which also appeared in HPLC analysis of the other Ergo stocks. Furthermore, the ratio of the area of P8.0 and P11.7 to P14.6 was compared for three different Ergo stocks (Fig. 12).

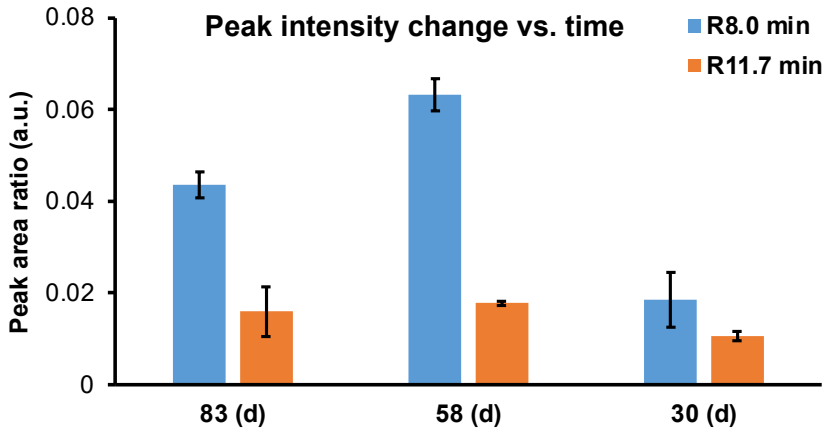

Figure 12: *Plot comparing ratio of P8.0 (205 nm) and P11.7 (205 nm) to P14.6 (281 nm) of ergosterol (Ergo) stocks. Ratio of 8.0 min (R8.0) and 11.7 min (R11.7) was calculated by taking the mean ± standard deviation (n = 3) for each Ergo stock. The age of stock (d) was calculated by subtracting the manufacture date of the stock from the date of the experiment. Peaks and retention times were obtained in high-performance liquid chromatography (HPLC), using 10 % H_2O/90 % solvent mixture (ACN:MeOH, 99:1) as eluent and recording at 205 nm and 281 nm.*

The graph reveals that the newest Ergo stock had the lowest amount of side constituents, suggesting that sterol stock stability presents a problem. For DHChol, the decline of IC_{50} values over the age of the stock was less pronounced.

3.1.2 Influence of antimycin A on J774 viability

Possible drug targets in kinetoplastids such as *Leishmania* are mitochondria, thus why, the mitochondrial inhibitor antimycin A was introduced as a reference compound. Typical examples of viability-concentration curves of AA for J774 are shown in Figure 13. During the viability assays for J774 cells with AA, no total inhibition of cell viability was obtained up to concentrations of 40 µM.

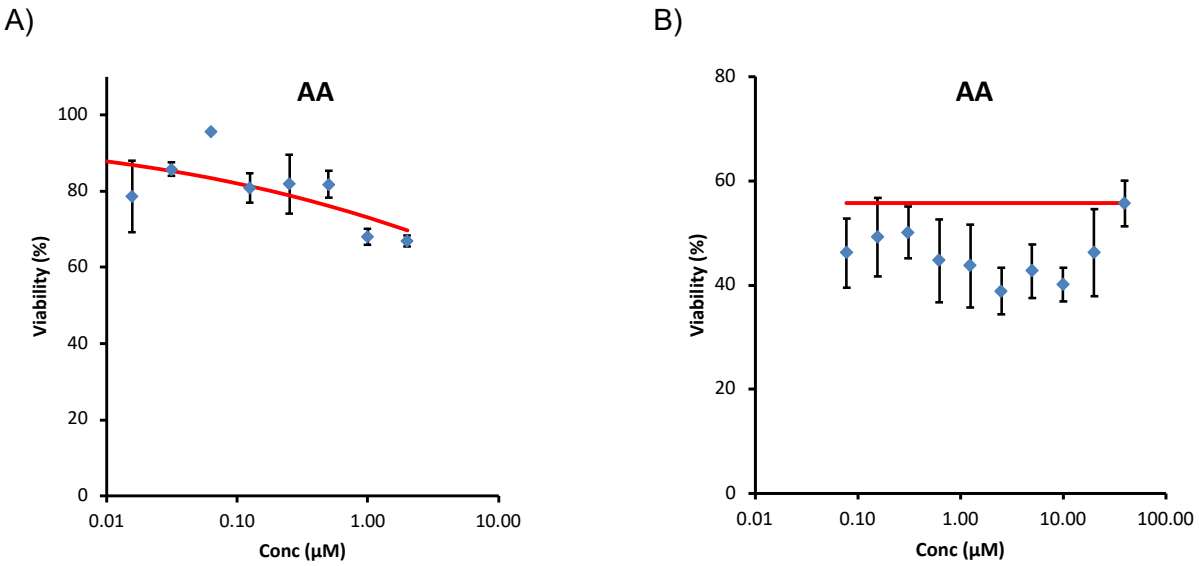

Figure 13: *Typical example of horizontal viability assay of J774 cells with different concentrations of antimycin A (AA). Concentrations (Conc) ranged from 0.001 µM–2 µM for (A) and 0.078 µM–40 µM for (B). Viability-concentration curves were established from a single culture batch calculating each data point by taking the mean ± standard deviation of wells (n = 2). Due to the incomplete inhibition, no IC_{50} values were calculated.*

This suggests that even in high concentrations, AA is unable to totally kill J774 cells.

3.2 Influence of different antioxidants on sterol EP antileishmanial activity

EPs were suggested to produce radicals as part of their antileishmanial mechanism. Therefore, antioxidants should influence their antileishmanial activity. To further investigate the mechanism of sterol EP action on *Leishmania,* antioxidants and radical scavengers were

introduced and hence IC_{50} values of antileishmanial compounds were studied in the presence and absence of antioxidants. To test this theory, the radical scavengers NAC, BHT and Trolox were used. At first, the influence of NAC, BHT and Trolox on LtP viability was tested. The means of IC_{50} values are displayed in Table 3.

Table 3: *IC_{50} values of antioxidants measured in horizontal viability assays in a total of 3–4 cell batches. Values were calculated by taking the mean ± standard deviation (SD) (n = 3) with concentrations ranging from 0.977 µM–2000 µM for N-acetyl cysteine (NAC), 0.098 µM–200 µM for butylated hydroxytoluene (BHT) and 0.098 µM–200 µM for 6-hydroxy-2,5,7,8-tetramethylchroman-2-carboxylic acid (Trolox).*

Compound	IC_{50} (µM) mean ± SD
NAC	>2000 µM
BHT	34 ± 11
Trolox	>200 µM

According to the results in Table 3, antioxidants for the interference assays were applied at the following concentrations: NAC 2000 µM; BHT 10 µM; Trolox 200 µM. Then vertical viability assays were performed, testing the antileishmanial effect of compounds in the absence and presence of antioxidants on the same 96-well plate. A typical example of a viability-concentration curve for Art in both presence and absence of NAC is shown in Figure 14.

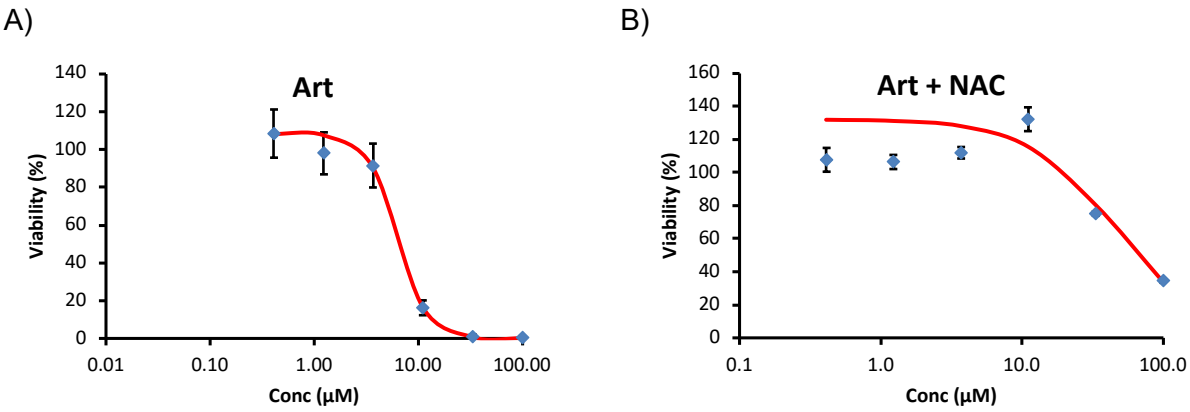

Figure 14: *Typical example of LtP viability (%) influenced by artemisinin (Art) in presence and absence of N-acetyl cysteine (NAC). Concentrations (Conc) of Art ranged from 0.41 µM–100 µM. The viability-concentration curve in absence of NAC is shown in (A) and upon addition of NAC (2 mM) in (B). Viability-concentration curves were established using a vertical viability assay from a single culture batch and calculating each data point by taking the mean ± standard deviation (n = 2), resulting in IC_{50} values of 6.32 µM ± 0.49 for (A) and 46 µM ± 16 for (B) and an overall change of the IC_{50} value of 729 %.*

The viability-concentration curves in Figure 14 demonstrate that the antileishmanial activity of Art is reduced in presence of NAC.

Analogous experiments were performed from 2–3 cell batches at different weeks with antioxidants and antileishmanial compounds. The averaged relative changes (%) of the IC_{50} values (obtained from the IC_{50} value in the presence of antioxidants divided by the IC_{50} value without antioxidants multiplied by 100) are shown in Table 4.

Table 4: *Relative change of mean IC_{50} values (%) ± standard deviation (SD) upon addition of antioxidant. The relative changes of IC_{50} values after treatment with N-acetyl cysteine (NAC, 2 mM), butylated hydroxytoluene (BHT, 10 µM) and 6-hydroxy-2,5,7,8-tetramethylchroman-2-carboxylic acid (Trolox, 200 µM) were calculated after performing vertical viability assays from 2–3 cell batches over 2–3 weeks. Concentrations of the tested compounds ranged from 0.82 µM–200 µM for ergosterol endoperoxide (ErgoEP) and dehydrocholesterol endoperoxide (DHCholEP), 0.01 µM–3 µM for amphotericin B (AmpB) and 0.41 µM–100 µM for artemisinin (Art).*

Compound	Relative change of IC_{50} (%), mean ± SD		
	with NAC	with BHT	with Trolox
ErgoEP	124 ± 20	46 ± 5	49 ± 30
DHCholEP	93 ± 4	117 ± 46	65 ± 27
AmpB	554 ± 80	142 ± 26	77 ± 3
Art	656 ± 96	144 ± 2	145 ± 25

It is noticeable that in the presence of NAC, the antileishmanial activity of AmpB and Art (as positive control compounds) strongly decreased, while IC_{50} values of ErgoEP and DHCholEP remained almost unchanged (around 100 %). For BHT, IC_{50} values for AmpB and Art are slightly increased, while for DHCholEP no change and ErgoEP even a decrease was noted. Although Trolox increased IC_{50} values for Art, it did not impair the action of the other compounds in LtP.

3.3 HPLC analysis of sterols

Since the results of antioxidant interference assays did not provide strong support for the idea that sterol EPs simply act via radical formation in LtP, an alternative hypothesis was tested. It is known that sterol EPs share structural similarities with endogenously found sterols in LtP. To study the influence of sterol EPs on endogenous sterol production in LtP, a LtP batch incubation method and an HPLC analysis was established. In the HPLC analysis, a C8

reversed-phase column and 10 % H_2O/90 % solvent mixture (ACN:MeOH, 99:1) as an eluent was used. Chromatographic traces were recorded in the 205 nm and 281 nm channels using a dual-channel UV detector.

For the established HPLC method, the retention times and ratios between peak areas of reference compounds were recorded in the reversed-phase HPLC system in previous studies (Table 5). The retention times can slightly vary which is why the area ratios of the peaks are demonstrated as an additional factor to differentiate the compounds and identify sterols with conjugated double bonds, such as Ergo, DHChol and 5-DHE.

Table 5: *Elution of sterols and related compounds in reversed-phase high-performance liquid chromatography analysis. Retention times (RT, min) and ratios between peak areas detected at the respective retention time in the 281 nm and 205 nm channels. Chromatograms were obtained from pure standard compounds or NMR-characterized fractions in previous studies. Compounds were cholesterol (Chol), ergosterol (Ergo), 7-dehydrocholesterol (DHChol), 5-dehydroepisterol (5-DHE), ergosterol endoperoxide (ErgoEP), dehydrocholesterol endoperoxide (DHCholEP), dehydroergosterol endoperoxide (DHErgoEP) and tetradehydrocholesterol endoperoxide (TDHCholEP).*

Compound	RT (min)	Area ratio A281 nm/A205 nm
TDHCholEP	6.2	0.095
DHErgoEP	6.4	0.024
DHCholEP	6.9	0.016
ErgoEP	7.1	0.007
5-DHE	12.2	5.864
DHChol	14.3	3.450
Ergo	14.6	1.971
Chol	18.5	0.000

To study the sterol EP influence on LtP, LtP culture batches (15 mL per sample) were incubated with different concentrations of sterol EPs, using the corresponding amount of EtOH (vehicle for sterol EP) in control samples. To monitor LtP growth, aliquots were taken, and the cell number was measured photometrically at 600 nm.

A typical growth curve with different concentrations of ErgoEP compared to a control sample incubated with EtOH is shown in Figure 15.

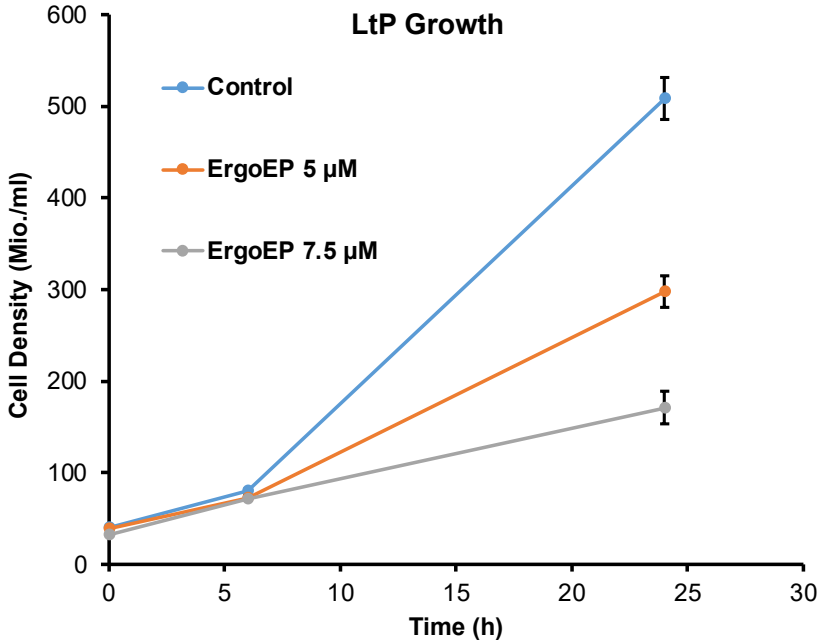

Figure 15: *Typical growth curve of LtP incubated with ergosterol endoperoxide (ErgoEP). Different concentrations of ErgoEP ranged from 5 µM to 7.5 µM. LtP samples treated with 7.5 µL ethanol were used as a control. Each data point represents the mean cell density (Mio/ml) ± standard deviation (n = 3) measured photometrically at 600 nm. Samples were measured after 0, 6 and 24 hours.*

The graph in Figure 15 verifies the inhibitory effects of ErgoEP on LtP. After subsequent preparation of the LtP cell pellets for each sample, saponification, solvent extraction with hexane, evaporation and redissolution in ACN, HPLC chromatograms of extracts were recorded. Typical chromatograms of a control sample only treated with EtOH are displayed in Figure 16. To improve the visibility of the peaks, the y-axis of the two chromatograms was differently scaled.

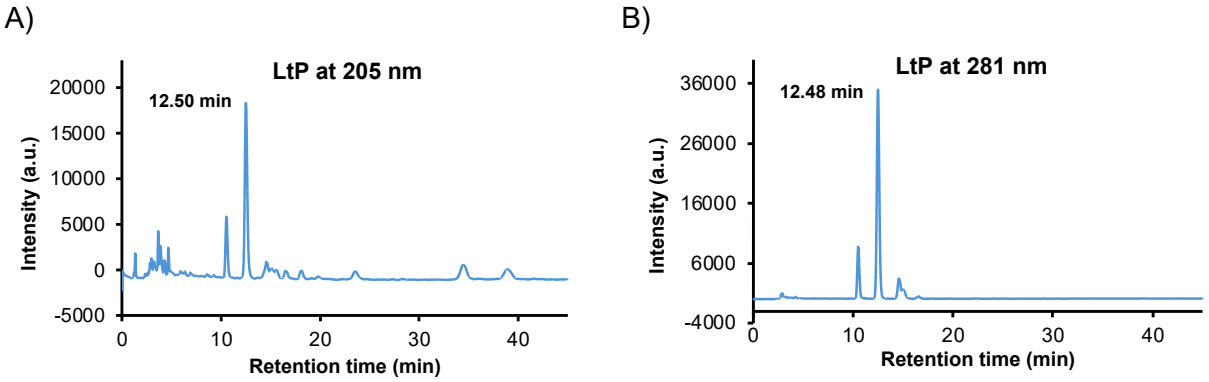

Figure 16: *Typical chromatogram of an extract from a saponified LtP pellet. The sample was treated with 6.25 µL ethanol (control), using 10 % H_2O/90 % solvent mixture (ACN:MeOH, 99:1) as eluent, and recorded at 205 nm and 281 nm. The retention times of the peaks of the major sterol 5-DHE are shown.*

The major peak at 12.50/12.48 min shown in Figure 16 can be identified as 5-dehydroepisterol (5-DHE) (see Table 5). To explore the influence of sterol EP in sterol production on LtP, the wet weight proportion (%) of 5-DHE equivalents of LtP samples treated with different concentrations of ErgoEP was determined (Fig. 17). ErgoEP treated samples were compared to a control group incubated with EtOH.

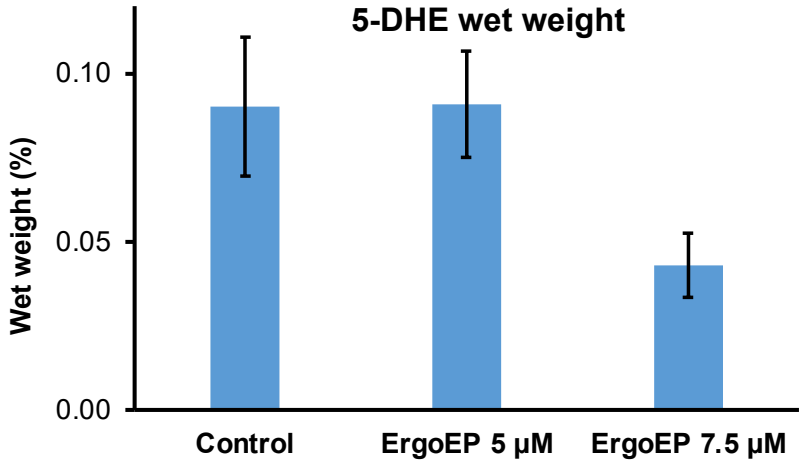

Figure 17: *Wet weight (%) of 5-dehydroepisterol (5-DHE) equivalents of LtP samples treated with ergosterol endoperoxide (ErgoEP). Concentrations of ErgoEP ranged from 5 µM–7.5 µM and the control sample was treated with 7.5 µL ethanol. Wet weight was calculated as mean ± standard deviation of 3 samples (n = 3).*

For DHCholEP analogous experiments were performed with different concentrations. A typical growth curve of LtP in the presence of DHCholEP compared to a control sample incubated with EtOH is displayed in Figure 18.

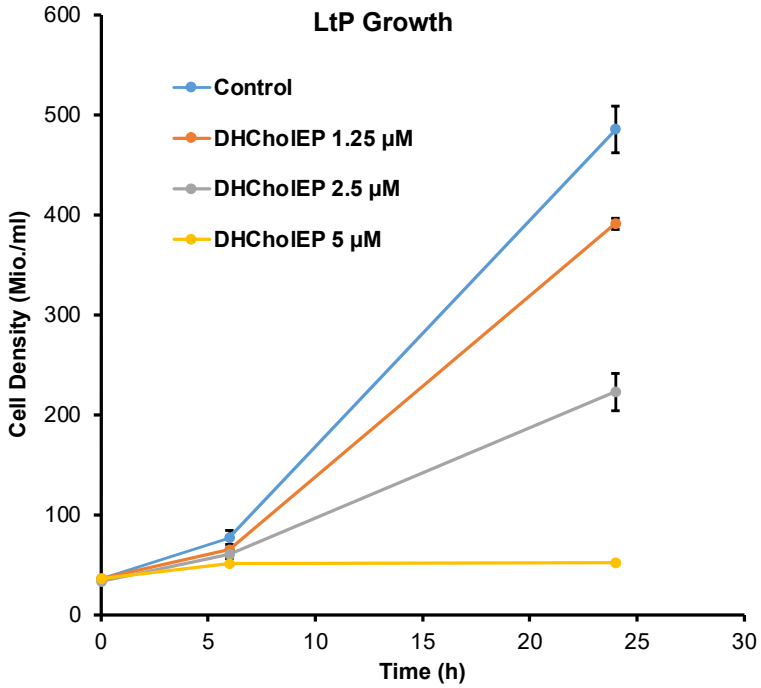

Figure 18: *Typical growth curve of LtP incubated with dehydrocholesterol endoperoxide (DHCholEP). Concentrations of DHCholEP ranged from 1.25 µM to 2.5 µM to 5 µM. LtP samples treated with 5 µL ethanol were used as a control. Each data point represents the mean cell density (Mio/ml) ± standard deviation (n = 3), measured photometrically at 600 nm. For DHCholEP 5 µM, the standard deviation was almost zero and is, therefore, not displayed. Samples were measured after 0, 6 and 24 hours.*

Inhibitory effects of DHCholEP on LtP growth are visible in Figure 18.

The wet weight (%) of 5-DHE equivalents of LtP samples treated with different concentrations of DHCholEP was also determined (Fig. 19). DHCholEP-treated samples were compared to a control group incubated with EtOH. Due to low cell yields, the samples treated with 5 µM DHCholEP were pooled together.

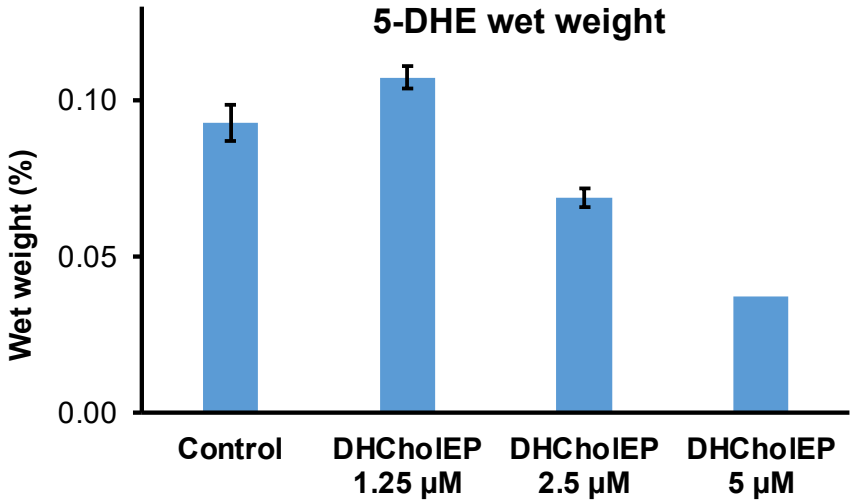

Figure 19: *Wet weight (%) of 5-dehydroepisterol (5-DHE) equivalents of LtP samples treated with dehydrocholesterol endoperoxide (DHCholEP). Concentrations of DHCholEP ranged from 1.25 µM to 2.5 µM and 5 µM. The control sample was treated with 5 µL ethanol. Wet weight was calculated as mean ± standard deviation (n = 3 for 1.25 µM and 2.5 µM, n = 1 for 5 µM) of three samples. For DHCholEP 5 µM, the cell yield was too low and therefore, the pellets were pooled together.*

As expected, the bar graph in Figure 19 shows a decrease in the 5-DHE wet weight (%) of the samples. Experiments with both sterol EPs demonstrate that they inhibit sterol synthesis in LtP parallel to their effect on LtP growth.

3.3.1 Evaluation of corticosterone as extraction standard

The so-far established HPLC method refers the peak area for 5-DHE to the wet weight of the LtP pellet. Variable losses during liquid-liquid extraction are not taken into account, leading to higher sample deviations in the final result and ultimately, not being able to measure smaller concentrations changes of the compound.

To counteract these effects and further improve the method, employing a potential internal standard could be of interest. Therefore, CCS, an adrenal cortex-produced glucocorticoid, was tested. In the first step, the UV spectrum of CCS (100 µM in EtOH) was detected in the range of 200 nm to 370 nm (Fig. 20). The maximum optical density of CCS was measured at 241 nm.

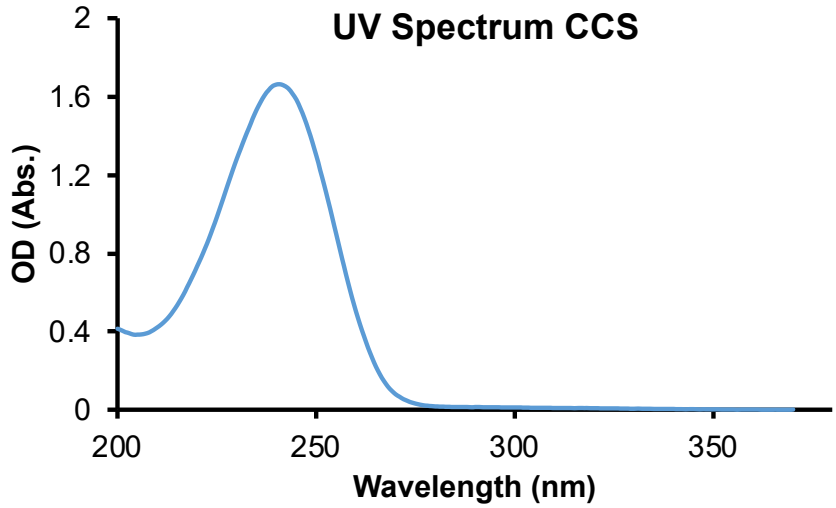

Figure 20: *UV spectrum of corticosterone (CCS) measured from 200 nm to 370 nm. 5 µL CCS (20 mM) was solved in 1000 µL ethanol and measured in quartz glass cuvettes using 1000 µL ethanol as a reference. The maximum of the optical density was reached at 241 nm.*

Furthermore, CCS (500 µM) was solved in ACN and analyzed in HPLC at 205 nm, 241 nm (first 5 min) and 281 nm (Fig. 21).

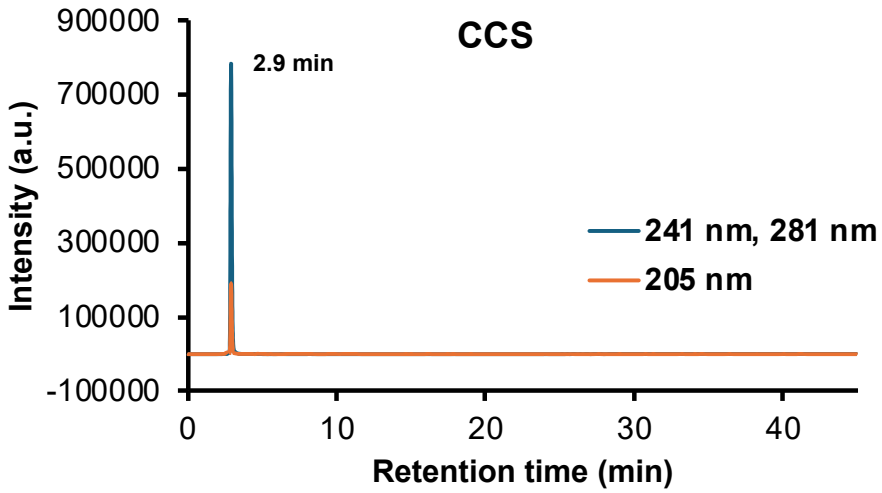

Figure 21: *HPLC chromatogram of corticosterone (CCS). 10 % H_2O/90 % solvent mixture (ACN:MeOH, 99:1) was used as eluent and sample was analyzed at 205 nm, 241 nm (first 5 min) and 281 nm. The sample contained 500 µM CCS solved in acetonitrile. Relevant peak at 2.9 min is shown.*

The chromatogram reveals that the peaks of CCS appear at 2.9 min and, therefore, do not interfere with the ones of LtP and synthetic EPs (see Table 5). Hence, it could be suitable as a standard.

However, even after several HPLC runs with 250 µM CCS (20 mM) in the hexane extraction

solution for LtP pellets, the peak of CCS was not detected. To analyze this problem, experiments studying differently treated samples of 250 µM CCS in hexane were performed (Fig. 22). In the first sample, 250 µM CCS was solved in only ACN. For the second sample, 250 µM CCS was dissolved in hexane, then the hexane was evaporated under a stream of N_2 and reconstituted with the corresponding amount of ACN. In the third sample type, the hexane with 250 µM CCS was shaken with saponification solution (omitting the KOH), and the subsequently extracted hexane was removed and redissolved in ACN. The fourth sample was prepared in the same way as the third but with KOH in the saponification solution.

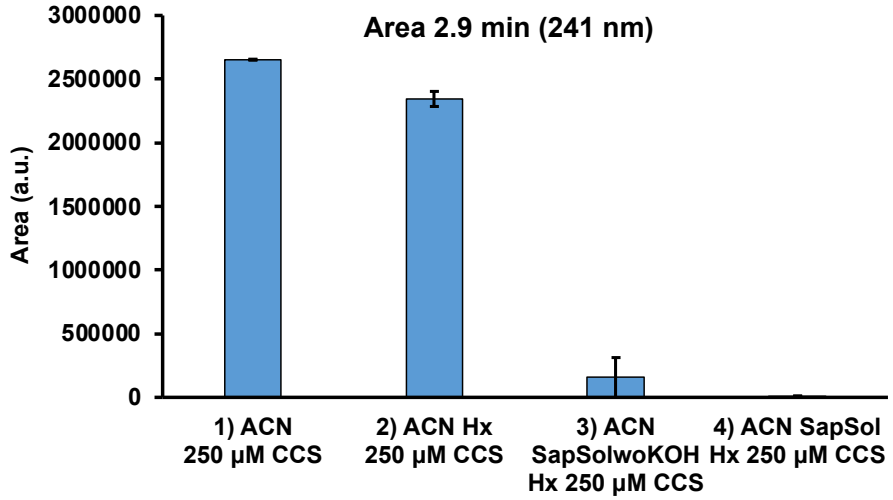

Figure 22: *Comparison of the area (a.u.) at 2.9 min (241 nm) between differently treated samples of corticosterone (CCS). (1) 250 µM CCS (20 mM) solved in 1.2 mL acetonitrile (ACN). (2) 250 µM CCS dissolved in 1.2 mL n-hexane (Hx), evaporated with N_2 and redissolved in 1.2 mL ACN. (3) 250 µM CCS mixed in 1.5 mL Hx with 0.5 mL H_2O and 1.5 mL saponification solution without potassium hydroxide (SapSolwoKOH, 35 % H_2O/65 % EtOH, without KOH), vortexed and then 1.2 mL of the hexane layer was taken and evaporated and finally, redissolved in 1.2 mL ACN (4) Treated the same way as (3) but with KOH in the saponification solution. Samples were analyzed with high-performance liquid chromatography with 10 % H_2O/90 % solvent mixture (ACN:MeOH, 99:1) as eluent and recorded at 205 nm, 241 nm and 281 nm. The mean ± standard deviation (n = 2) was calculated.*

These experiments reveal that CCS vanishes during treatment with saponification solution, especially when containing KOH.

4. Discussion

Leishmaniasis and its treatment pose significant global health challenges, likely to persist for decades. The complexity of the disease is attributed to the multitude of *Leishmania* species worldwide and their variable clinical manifestations in patients. The expansion of the endemic areas for the vector, the sand fly, coupled with potential alternative hosts may exacerbate the situation (McGwire and Satoskar 2014).

This includes increased contact between humans and other mammals with the vector and the substantial reservoir of infected dogs in the Mediterranean basin. Treatment complications arise not only from the disease itself but also from pharmacological interventions and socioeconomic factors in endemic regions (Valero and Uriarte 2020). The disease is particularly complex compared to other microbiological infections because the pathogens reside within host macrophages, hiding from the immune system and complicating treatment (Kaye and Scott 2011). Challenges with effective antileishmanial drugs include resistance to antimonials in India and the fact that certain treatments, although effective, are either expensive or require clinical settings for administration, such as miltefosine and liposomal amphotericin B (Feng et al. 2022). Socioeconomic barriers may hinder the eradication of leishmaniasis in specific world regions, underscoring the need for new antileishmanial compounds (Valero and Uriarte 2020).

ErgoEP, an ingredient found in certain mushrooms, has been studied for its biological activities for several years (Merdivan and Lindequist 2017). However, its application as an antileishmanial agent has not been specifically investigated. Another related compound is DHCholEP. Both compounds are derived from triene sterols, which possess two conjugated double bonds in the B-ring of the sterol structure, enabling them to incorporate singlet oxygen to form EPs. Little is known about the biological activities of DHCholEP (Wang et al. 2019). Previous theses have gathered some basic information about both sterol EPs. The present work aims to refine this knowledge and improve experimental methods for future studies. In the first part of the study, the activity of sterol EP against LtP (as a model for pathogenic *Leishmania*) and J774 macrophages (as a model for macrophage host cells) was compared. ErgoEP exhibited inhibitory effects on the viability of both LtP and J774 macrophages, as evidenced by the viability concentration curves shown in Figure 8. ErgoEP caused a significant decline in viability within a specific concentration range. However, much higher concentrations were required for J774 macrophages than for LtP to decline their viability.

DHCholEP elicited a quantitatively similar response in both cell types, albeit at slightly lower

concentrations in LtP, as depicted in Figure 9.
To obtain reliable data on the impact of sterol EP and related compounds on the viability of both cell types, these experiments were repeated across several cell batches throughout 5 to 7 weeks. The mean values and standard deviations of the obtained IC_{50} values are presented in Table 2. In addition to sterol EP, the test set included the parent sterols, Pen, AmpB, and Mil as antileishmanial agents, KetoAz, ItraAz, MiAz as antifungal agents, Art as another natural endoperoxide, and AA as a mitochondrial inhibitor.

Based on the experimental IC_{50} values in both cell types, a selectivity factor was calculated. Notably, even established antileishmanial compounds such as Pen, AmpB, and Mil exhibited considerable variability in selectivity factors. This variability suggests that our straightforward comparison may not encompass all potential antileishmanial activities *in vivo*, given that Pen is recognized as an effective agent against cutaneous leishmaniasis. It implies that antileishmanial activities, particularly those that interfere with host-pathogen interactions involving intracellular *Leishmania* amastigotes within host macrophages, are likely not identified by this assay type. Nonetheless, such data can aid in selecting compounds for evaluation in more complex model systems and *in vivo* tests. Among antifungal agents, the low IC_{50} values in LtP are noteworthy. Consequently, additional testing in more advanced model systems could determine the potential of repurposing these drugs against leishmaniasis.

The natural endoperoxide Art demonstrated activity against LtP with IC_{50} values in the micromolar range (6.2 µM, see Table 2), yet it also exhibited some toxicity against J774 macrophages (IC_{50} = 17 µM), resulting in a relatively modest selectivity factor (SF = 3). In previously published work, IC_{50} values of 2.96 µM for Art for LtP and 192 µM for J774 macrophages were reported (Geroldinger et al. 2018). Although the activity against LtP was comparable in the previous study, it was less toxic against J774 macrophages. This discrepancy suggests that revisiting experimental factors, including the age of stock solutions, could be beneficial.
The mitochondrial inhibitor AA yielded an IC_{50} value in LtP of approximately 1.755 µM, as indicated in Table 2. In J774 macrophages, it was not possible to ascertain a precise IC_{50} value for AA, even at the highest tested concentration of 40 µM, the viability of J774 cells could not be reduced by more than about 50 %, as shown in Figure 13. This observation suggests that macrophage host cells possess significant resistance to compounds that induce ROS

formation, like AA. However, AA revealed its efficacy against *Leishmania* despite the rapid development of resistance, posing a challenge for the use of AA in this context (Schnaufer et al. 2000).

For sterol EPs, IC_{50} values in the low micromolar range were determined in *Leishmania*, while for J774 macrophages, the IC_{50} values were generally 5 to 8 times higher, as shown in Table 2. This indicates a degree of selectivity for *Leishmania* over macrophages in our simplified test system. Notably, the IC_{50} values of the sterol EPs were lower compared to their parent sterols, implying that the endoperoxide group increases antileishmanial activity.

It was observed that the IC_{50} values for Ergo (and to a lesser extent for DHChol) decreased over time with aged stock solutions, as depicted in Figure 10, suggesting an apparent increase in antileishmanial activity of these Ergo stocks over time. To investigate this unexpected behavior further, the stock solutions of Ergo at various ages were analyzed using HPLC, as presented in Figure 11. Although the peak area of Ergo in the 281 nm channel consistently exceeded 95 % of all peak areas (in this channel), additional small peaks in the 205 nm channel were noted that varied with the age of the stock solution, particularly a peak around 8 min that was significantly higher in aged solutions than in new ones, as illustrated in Figure 12. While we have not yet identified the chemical compound responsible for these peaks, it is well-established that minor components can exhibit significant pharmacological activity. It could be possible that after a certain time the Ergo stocks partially oxidated or hydrolyzed to degradation products different from known endoperoxides and therefore, experienced an increase in their antileishmanial activity. As a practical measure, new stock solutions of Ergo and DHChol were prepared every 3 to 4 weeks.

Building on the observation that sterol EPs exhibited greater antileishmanial activity than their parent sterols, and considering previous findings (Schrödl 2023) that these EPs can generate radicals, we evaluated the impact of antioxidants on antileishmanial activity in the LtP model system. Extending prior research, NAC, BHT, and Trolox were tested as antioxidants. Initially the effects of these antioxidants on *Leishmania* were assessed, as documented in Table 3, revealing that NAC and Trolox were tolerated in LtP at concentrations exceeding 2000 µM and 200 µM, respectively. In contrast, BHT displayed an IC_{50} value of approximately 34 µM.

Subsequently, the interactions of NAC at 2000 µM, Trolox at 200 µM, and BHT at 10 µM with

the antileishmanial activity of sterol EPs and related compounds were investigated. Figure 14 shows a positive control, illustrating the modulation of the IC_{50} value of Art by NAC. The IC_{50} value of Art significantly increased in the presence of NAC.
Experimental data from all compounds, tested in triplicate, is summarized in Table 4. Notably, NAC had a significant effect on AmpB and Art, suggesting that radical formation plays a role in their antileishmanial mechanism and can be counteracted by NAC. However, the effects of BHT and Trolox differed quantitatively from those of NAC. While BHT showed a weaker effect compared to NAC, Trolox impaired the activity of Art but not of AmpB, making the results with BHT and Trolox more challenging to interpret. However, the lower concentration of BHT could be a possible reason for its low effect.
Regarding sterol EPs, it was observed that NAC marginally, if at all, increased the IC_{50} values, indicating that although sterol EPs have the ability to form radicals, this mechanism contributes only partially to their antileishmanial activity.

To investigate an alternative mechanism of action for sterol EP, the production of endogenous sterols in *Leishmania* and their modulation by sterol EP was analyzed. Given the structural similarity between sterol EP and *Leishmania*'s endogenous sterols, it is plausible that the EP may disrupt the biosynthesis of *Leishmania* sterols. Using data from previous studies and commercially available standards, a table detailing retention times and absorption ratios in the 281 nm and 205 nm channels of HPLC analysis for known sterol derivatives was compiled (Table 5). This data enabled us to assign chromatographic peaks from LtP extracts within an approximate time window of 0.2 min. To assess the impact of sterol EP on LtP growth and sterol biosynthesis, incubations with 15 mL LtP cultures at various concentrations around the IC_{50} value were conducted, alongside control samples containing only the vehicle (EtOH).
During the 24 h incubation period, the growth of the samples was measured (after 0, 6 and 24 h), as depicted in Figures 15 (ErgoEP) and 18 (DHCholEP). The data indicates that the growth of LtP can be significantly slowed or even halted at the tested concentrations. Post-incubation, cell pellets were prepared and subjected to HPLC analysis. The chromatograms of a control group containing EtOH, presented in Figure 16, reveal a major peak in the 281 nm channel at approximately 12.48 min, corresponding to 5-DHE, which is the predominant sterol in LtP, unlike many other microorganisms where Ergo is the dominant sterol (Braga 2019). Quantitative analysis of 5-DHE in LtP samples treated with sterol EP showed a consistent decrease in 5-DHE levels with increasing concentrations of sterol EP (Fig. 17 ErgoEP; Fig. 19 DHCholEP). This suggests that sterol EP may disrupt the sterol biosynthesis pathway in LtP

or other related pathways critical for sterol biosynthesis.

The established method for sterol analysis involves multiple steps, including saponification, liquid-liquid extraction, solvent evaporation, and reconstitution with ACN, making the final reported percentage of 5-DHE, based on the wet weight of *Leishmania*, prone to various sources of error. To enhance accuracy, the addition of CCS as an internal standard was explored (Chiocchio and Matkovic 2011). Initially, the UV spectra of CCS (Fig. 20) were measured, noting an absorption maximum at 241 nm. HPLC analysis of a CCS aliquot dissolved in ACN yielded a chromatogram with a peak at 2.9 min (Fig. 21), which does not overlap with other sterol intermediates found in LtP extracts and synthetic EPs (see Table 5). For increased sensitivity, the HPLC detector could be temporarily (first 5 min) switched from the 281 nm to the 241 nm channel. Further analysis of CCS during various extraction steps revealed a significant reduction in CCS, particularly when 250 µM of CCS was dissolved in the hexane extraction phase containing the saponification solution (Fig. 22). Future studies should further assess whether CCS is suitable as an internal standard for LtP pellet extraction or if higher concentrations are required to prevent loss during extraction.

In conclusion, this study has demonstrated the antileishmanial activity of sterol EP and their selective efficacy for LtP over J774 cells. The mechanism of action against *Leishmania* involves not only radical-mediated effects but also potentially the inhibition of endogenous sterol synthesis. Furthermore, this work provides valuable insights into how current experimental procedures might be refined.

5. Summary

Leishmaniasis is an infectious tropical disease caused by *Leishmania* parasites (protozoa), affecting at least two million people annually in 98 subtropical and tropical countries. It manifests in three forms: cutaneous, mucocutaneous, and visceral, each with varying severity. The disease is transmitted by infected female sand flies, injecting the motile flagellated promastigotes into hosts during blood meals. Inside host macrophages, the parasites transform into non-flagellated amastigotes and proliferate, evading the immune system. Increasing drug resistance and adverse effects of current treatments necessitate new antileishmanial drugs. Endoperoxides (EP) are promising candidates, having shown antileishmanial activity and being used as antimalarial agents. Their efficacy and mode of action depend on their structure beyond the EP group, which is of interest for drug development. Therefore, this thesis aimed to evaluate (i) the impact of sterol endoperoxides (ergosterol endoperoxide (ErgoEP), dehydrocholesterol endoperoxide (DHCholEP)) on the viability of *Leishmania tarentolae* promastigotes (LtP) and J774 murine macrophages, (ii) the effect of antioxidants (N-acetyl cysteine (NAC), butylated hydroxytoluene (BHT), 6-hydroxy-2,5,7,8-tetramethylchroman-2-carboxylic acid (Trolox)) on the viability of LtP treated with sterol EP, (iii) the influence of sterol EP on sterol synthesis in LtP and (iv) possible improvements of sterol analysis in LtP.

To investigate these questions, viability assays of LtP and J774 were executed in 96-well plates and after 48 h incubation with substances, resazurin fluorescence was used to obtain corresponding IC_{50} values. To assess the impairment of antileishmanial viability of the substances by the antioxidants NAC, BHT and Trolox, alterations in IC_{50} values were recorded upon addition of said antioxidants. After incubation of LtP with ErgoEP and DHCholEP, sterol analysis was performed using high-performance liquid chromatography (HPLC) analysis. Furthermore, corticosterone (CCS) was evaluated as an internal standard for this type of analysis. The experiments revealed IC_{50} values in LtP vs. J774 for ErgoEP of 4.5 ± 1.2 µM vs. 22 ± 5 µM and for DHCholEP 2.0 ± 0.4 µM vs. 15 ± 5 µM. This indicates a selectivity factor of 5–8 for LtP over J774. For sterol EP actions on LtP, no major influence of antioxidants was observed. HPLC analysis demonstrated that both sterol EPs inhibited the biosynthesis of the major sterol 5-dehydroepisterol in LtP and CCS could so far not be used as a standard due to losses during extraction. In conclusion, sterol EPs could be suitable as antileishmanial agents but further effectivity and mechanistic studies in more complex and *in vivo* model systems are required.

6. Zusammenfassung

Die tropische Infektionskrankheit Leishmaniose wird verursacht durch protozoische *Leishmanien*, die jährlich mindestens zwei Millionen Menschen in 98 Ländern betrifft. Die Krankheit hat drei Hauptformen: Kutane, mukokutane und viszerale Leishmaniose. Infizierte, weibliche Sandmücken übertragen die Promastigoten durch Blutmahlzeiten auf Menschen und Tiere, wo sie in den Makrophagen zu Amastigoten differenzieren. Anlässlich ihrer Fähigkeit sich in den Makrophagen zu verstecken, entgehen *Leishmanien* dem Abwehrmechanismus des Immunsystems. Aufgrund zunehmender Resistenzen und Nebenwirkungen bestehender Behandlungen ist die Entwicklung neuer antileishmanialer Medikamente erforderlich. Eine Klasse von Arzneimittelkandidaten sind Endoperoxide (EP), die antileishmaniale Wirkung gezeigt haben und bereits als Malariamittel eingesetzt werden. Ihre Wirkungsweise und Effektivität hängen jedoch stark von der Struktur außerhalb der EP-Gruppe ab.

Ziel war es daher, (i) die Auswirkungen von Sterol-Endoperoxiden (Ergosterol-Endoperoxid (ErgoEP), Dehydrocholesterol-Endoperoxid (DHCholEP)) auf die Lebensfähigkeit von *Leishmania tarentolae Promastigoten* (LtP) und J774-Mausmakrophagen zu untersuchen, (ii) den Effekt von Antioxidantien (N-Acetylcystein (NAC), butyliertes Hydroxytoluol (BHT), 6-Hydroxy-2,5,7,8-tetramethylchroman-2-carbonsäure (Trolox)) auf die Sterol-EP Wirkung in LtP zu beobachten, (iii) den Einfluss von Sterol-EP auf die Sterolsynthese in LtP abzuklären und (iv) Verbesserungen der Sterol-Analyse zu testen. Um dies zu untersuchen, wurden Viabilitätstests von LtP und J774 in 96-Well-Platten nach 48 h Inkubation mit Substanzen mit Resazurin als Indikator durchgeführt und IC_{50}-Werte ermittelt. Die Verminderung der antileishmanialen Wirkung von Substanzen wurde nach der Zugabe von NAC, BHT und Trolox beurteilt. Nach der Inkubation von LtP mit ErgoEP und DHCholEP, wurden Sterol-Analysen mittels Hochleistungsflüssigkeitschromatographie (HPLC) durchgeführt. Ferner wurde Corticosteron (CCS) als interner Standard bei der Sterol-Analyse evaluiert. Die Experimente ergaben IC_{50}-Werte von 4.5 ± 1.2 µM für ErgoEP in LtP und 22 ± 5 µM in J774. DHCholEP erreichte IC_{50}-Werte von 2.0 ± 0.4 µM in LtP und 15 ± 5 µM in J774 mit einem Selektivitätsfaktor von 5–8 für LtP gegenüber J774. Es wurde kein wesentlicher Einfluss von Antioxidantien auf die Wirkung von Sterol-EPs in LtP beobachtet. HPLC-Analysen zeigten, dass Sterol-EPs das Hauptsterol 5-Dehydroepisterol in LtP hemmten, während CCS aufgrund von Extraktionsverlusten nicht als Standard verwendet werden konnte. Daher steht fest, dass Sterol-EPs als antileishmaniale Wirkstoffe geeignet sein könnten, jedoch weitere Studien in komplexeren und *in vivo* Modellsystemen erforderlich sind.

7. Abbreviations

5-DHE	5-Dehydroepisterol
AA	Antimycin A
ACN	Acetonitrile
AmpB	Amphotericin B
Art	Artemisinin
BHI	Brain heart infusion medium
BHT	Butylated hydroxytoluene
CCS	Corticosterone
Chol	Cholesterol
Conc	Concentration
DHChol	7-Dehydrocholesterol
DHCholEP	Dehdyrocholesterol endoperoxide
DHErgoEP	Dehydroergosterol endoperoxide
DMEM	Dulbecco's modified eagle's medium
DMSO	Dimethyl sulfoxide
EDF tube	Eppendorf tube
EP	Endoperoxide
Ergo	Ergosterol
ErgoEP	Ergosterol endoperoxide
EtOH	Ethanol
FCS	Fetal calf serum
HIV	Human immunodeficiency virus
HPLC	High-performance liquid chromatography
Hx	n-Hexane
IC_{50}	Half maximal inhibitory concentration
ItraAz	Itraconazole
KetoAz	Ketoconazole
KOH	Potassium hydroxide
LtP	*Leishmania tarentolae* promastigotes
MeOH	Methanol
MiAz	Miconazole
Mil	Miltefosine

NAC	N-acetyl cysteine
OD	Optical density
PBS	Phosphate-buffered saline
Pen	Pentamidine
ROS	Reactive oxygen species
SD	Standard deviation
TDHCholEP	Tetradehydrocholesterol endoperoxide
Trolox	6-Hydroxy-2,5,7,8-tetramethylchroman-2-carboxylic acid
Viab	Viability
Ye	Yeast extract
YEM	Yeast extract medium

8. References

Alpizar-Sosa EA, Ithnin NRB, Wei W, Pountain AW, Weidt SK, Donachie AM, Ritchie R, Dickie EA, Burchmore RJS, Denny PW, et al. 2022. Amphotericin B resistance in Leishmania mexicana: Alterations to sterol metabolism and oxidative stress response. PLOS Neglected Tropical Diseases, 16(9):e0010779.

Alven S, Aderibigbe BA. 2020. Nanoparticles formulations of artemisinin and derivatives as potential therapeutics for the treatment of cancer, leishmaniasis and malaria. Pharmaceutics, 12(8):748.

Bandi C, Mendoza-Roldan JA, Otranto D, Alvaro A, Louzada-Flores VN, Pajoro M, Varotto-Boccazzi I, Brilli M, Manenti A, Montomoli E, et al. 2023. Leishmania tarentolae: a vaccine platform to target dendritic cells and a surrogate pathogen for next generation vaccine research in leishmaniases and viral infections. Parasites & Vectors, 16(1):35.

Bolhassani A, Taheri T, Taslimi Y, Zamanilui S, Zahedifard F, Seyed N, Torkashvand F, Vaziri B, Rafati S. 2011. Fluorescent Leishmania species: Development of stable GFP expression and its application for in vitro and in vivo studies. Experimental Parasitology, 127(3):637–645.

Braga SS. 2019. Multi-target drugs active against leishmaniasis: A paradigm of drug repurposing. European Journal of Medicinal Chemistry, 183:111660.

Cao L, Jiang W, Cao S, Zhao P, Liu J, Dong H, Guo Y, Liu Q, Gong P. 2019. In vitro leishmanicidal activity of antimicrobial peptide KDEL against Leishmania tarentolae. Acta Biochimica et Biophysica Sinica, 51(12):1286–1292.

Chiocchio V, Matkovic L. 2011. Determination of ergosterol in cellular fungi by HPLC. A modified technique. J. Argent. Chem. Soc., 98.

Elawad MA, Elkhalifa MEM, Hamdoon AAE, Salim LHM, Ahmad Z, Ayaz M. 2023. Natural products derived steroids as potential anti-leishmanial agents; disease prevalence, underlying mechanisms and future perspectives. Steroids, 193:109196.

Feng M, Jin Y, Yang S, Joachim AM, Ning Y, Mori-Quiroz LM, Fromm J, Perera C, Zhang K, Werbovetz KA, et al. 2022. Sterol profiling of Leishmania parasites using a new HPLC-tandem mass spectrometry-based method and antifungal azoles as chemical probes reveals a key intermediate sterol that supports a branched ergosterol biosynthetic pathway. International Journal for Parasitology: Drugs and Drug Resistance, 20:27–42.

Flannery AR, Renberg RL, Andrews NW. 2013. Pathways of iron acquisition and utilization in *Leishmania*. Current Opinion in Microbiology, 16(6):716–721.

Geroldinger G, Tonner M, Fudickar W, De Sarkar S, Dighal A, Monzote L, Staniek K, Linker T, Chatterjee M, Gille L. 2018. Activation of anthracene endoperoxides in Leishmania and impairment of mitochondrial functions. Molecules, 23(7):1680.

Gluenz E, Ginger ML, McKean PG. 2010. Flagellum assembly and function during the Leishmania life cycle. Current Opinion in Microbiology, 13(4):473–479.

Goto Y, Mizobuchi H. 2023. Pathological roles of macrophages in *Leishmania* infections. Parasitology International, 94:102738.

Goto Y, Ito T, Ghosh S, Mukherjee B. 2023. Access and utilization of host-derived iron by Leishmania parasites. Journal of Biochemistry, 175(1):17–24.

Gupta S, Nishi. 2011. Visceral leishmaniasis: Experimental models for drug discovery. The Indian Journal of Medical Research, 133(1):27–39.

Gurel MS, Tekin B, Uzun S. 2020. Cutaneous leishmaniasis: A great imitator. Clinics in Dermatology, 38(2):140–151.

Handler MZ, Patel PA, Kapila R, Al-Qubati Y, Schwartz RA. 2015. Cutaneous and mucocutaneous leishmaniasis: Clinical perspectives. Journal of the American Academy of Dermatology, 73(6):897–908.

He L, Shi W, Liu X, Zhao X, Zhang Z. 2018. Anticancer action and mechanism of ergosterol peroxide from Paecilomyces cicadae fermentation broth. International Journal of Molecular Sciences, 19(12):3935.

Karamysheva ZN, Moitra S, Perez A, Mukherjee S, Tikhonova EB, Karamyshev AL, Zhang K. 2021. Unexpected role of sterol synthesis in RNA stability and translation in Leishmania. Biomedicines, 9(6):696.

Kaye P, Scott P. 2011. Leishmaniasis: complexity at the host–pathogen interface. Nature Reviews Microbiology, 9(8):604–615.

Laranjeira-Silva MF, Hamza I, Pérez-Victoria JM. 2020. Iron and heme metabolism at the Leishmania-host interface. Trends in parasitology, 36(3):279–289.

Lee M-S, Bensinger SJ. 2022. Reprogramming cholesterol metabolism in macrophages and its role in host defense against cholesterol-dependent cytolysins. Cellular & Molecular Immunology, 19(3):327–336.

Li X, Wu Q, Bu M, Hu L, Du WW, Jiao C, Pan H, Sdiri M, Wu N, Xie Y, et al. 2016. Ergosterol peroxide activates Foxo3-mediated cell death signaling by inhibiting AKT and c-Myc in human hepatocellular carcinoma cells. Oncotarget, 7(23):33948–33959.

Machin L, Piontek M, Todhe S, Staniek K, Monzote L, Fudickar W, Linker T, Gille L. 2022. Antileishmanial anthracene endoperoxides: Efficacy in vitro, mechanisms and structure-activity relationships. Molecules (Basel, Switzerland), 27(20):6846.

Marquis J-F, Gros P. 2007. Intracellular Leishmania: your iron or mine? Trends in Microbiology, 15(3):93–95.

Mathur R, Das RP, Ranjan A, Shaha C. 2015. Elevated ergosterol protects *Leishmania* parasites against antimony-generated stress. The FASEB Journal, 29(10):4201–4213.

McCall L-I, El Aroussi A, Choi JY, Vieira DF, De Muylder G, Johnston JB, Chen S, Kellar D, Siqueira-Neto JL, Roush WR, Podust LM, McKerrow JH. 2015. Targeting ergosterol biosynthesis in Leishmania donovani: Essentiality of sterol 14alpha-demethylase. PLoS Neglected Tropical Diseases, 9(3):e0003588.

McGwire BS, Satoskar AR. 2014. Leishmaniasis: clinical syndromes and treatment. QJM: An International Journal of Medicine, 107(1):7–14.

Mendes A, Armada A, Cabral LIL, Amado PSM, Campino L, Cristiano MLS, Cortes S. 2022. 1,2,4-Trioxolane and 1,2,4,5-tetraoxane endoperoxides against old-world Leishmania parasites: In vitro activity and mode of action. Pharmaceuticals, 15(4):446.

Mendoza-Roldan JA, Votýpka J, Bandi C, Epis S, Modrý D, Tichá L, Volf P, Otranto D. 2022. *Leishmania tarentolae* : A new frontier in the epidemiology and control of the leishmaniases. Transboundary and Emerging Diseases, 69(5).

Merdivan S, Lindequist U. 2017. Ergosterol peroxide: A mushroom-derived compound with promising biological activities-A review. International Journal of Medicinal Mushrooms, 19(2):93–105.

Meshnick SR. 2002. Artemisinin: mechanisms of action, resistance and toxicity. International Journal for Parasitology, 32(13):1655–1660.

Mori T, Abe I. 2022. Structural basis for endoperoxide-forming oxygenases. Beilstein Journal of Organic Chemistry, 18:707–721.

Müllebner A, Patel A, Stamberg W, Staniek K, Rosenau T, Netscher T, Gille L. 2009. Modulation of the mitochondrial cytochrome bc1 complex activity by chromanols and related compounds. ACS Publications.

O'Neill PM, Posner GH. 2004. A medicinal chemistry perspective on artemisinin and related endoperoxides. Journal of Medicinal Chemistry, 47(12):2945–2964.

Pace D. 2014. Leishmaniasis. The Journal of Infection, 69 Suppl 1:S10-18.

Pastor J, García M, Steinbauer S, Setzer WN, Scull R, Gille L, Monzote L. 2015. Combinations of ascaridole, carvacrol, and caryophyllene oxide against Leishmania. Acta Tropica,

145:31–38.
Pearson RD, Wheeler DA, Harrison LH, Kay HD. 1983. The immunobiology of leishmaniasis. Clinical Infectious Diseases, 5(5):907–927.
Plastaras JP, Guengerich FP, Nebert DW, Marnett LJ. 2000. Xenobiotic-metabolizing cytochromes P450 convert prostaglandin endoperoxide to hydroxyheptadecatrienoic acid and the mutagen, malondialdehyde. Journal of Biological Chemistry, 275(16):11784–11790.
Podinovskaia M, Descoteaux A. 2015. Leishmania and the macrophage: a multifaceted interaction. Future Microbiology, 10(1):111–129.
Pucadyil TJ, Tewary P, Madhubala R, Chattopadhyay A. 2004. Cholesterol is required for Leishmania donovani infection: implications in leishmaniasis. Molecular and Biochemical Parasitology, 133(2):145–152.
Sasidharan S, Saudagar P. 2021. Leishmaniasis: where are we and where are we heading? Parasitology Research, 120(5):1541–1554.
Schnaufer A, Sbicego S, Blum B. 2000. Antimycin A resistance in a mutant Leishmania tarentolae strain is correlated to a point mutation in the mitochondrial apocytochrome b gene. Current Genetics, 37(4):234–241.
Schrödl EM. 2023. Antileishmanial mechanism of sterol endoperoxides: Influence on ergosterol synthesis. Vienna: University of Veterinary Medicine Vienna.
Serafim TD, Iniguez E, Oliveira F. 2020. Leishmania infantum. Trends in Parasitology, 36(1):80–81.
Singh R, Kashif M, Srivastava P, Manna PP. 2023. Recent advances in chemotherapeutics for leishmaniasis: Importance of the cellular biochemistry of the parasite and its molecular interaction with the host. Pathogens, 12(5):706.
Taslimi Y, Zahedifard F, Rafati S. 2018. Leishmaniasis and various immunotherapeutic approaches. Parasitology, 145(4):497–507.
Taylor VM, Muñoz DL, Cedeño DL, Vélez ID, Jones MA, Robledo SM. 2010. Leishmania tarentolae: Utility as an in vitro model for screening of antileishmanial agents. Experimental Parasitology, 126(4):471–475.
Tian N, Li C, Tian N, Zhou Q, Hou Y, Zhang B, Wang X. 2017. Syntheses of 7-dehydrocholesterol peroxides and their improved anticancer activity and selectivity over ergosterol peroxide. New Journal of Chemistry, 41(24):14843–14846.
Torres-Santos EC, Sampaio-Santos MI, Buckner FS, Yokoyama K, Gelb M, Urbina JA, Rossi-Bergmann B. 2009. Altered sterol profile induced in Leishmania amazonensis by a natural dihydroxymethoxylated chalcone. Journal of Antimicrobial Chemotherapy, 63(3):469–472.
Valero NNH, Uriarte M. 2020. Environmental and socioeconomic risk factors associated with visceral and cutaneous leishmaniasis: a systematic review. Parasitology Research, 119(2):365–384.
Varotto-Boccazzi I, Manenti A, Dapporto F, Gourlay LJ, Bisaglia B, Gabrieli P, Forneris F, Faravelli S, Bollati V, Rubolini D, et al. 2021. Epidemic preparedness—Leishmania tarentolae as an easy-to-handle tool to produce antigens for viral diagnosis: Application to COVID-19. Frontiers in Microbiology, 12:736530.
Wang Y, Tian N, Li C, Hou Y, Wang X, Zhou Q. 2019. Incorporation of 7-dehydrocholesterol into liposomes as a simple, universal and efficient way to enhance anticancer activity by combining PDT and photoactivated chemotherapy. Chemical Communications, 55(93):14081–14084.
Xu L, Korade Z, Porter NA. 2010. Oxysterols from free radical chain oxidation of 7-dehydrocholesterol: Product and mechanistic studies. Journal of the American Chemical Society, 132(7):2222–2232.
Yan J, Horng T. 2020. Lipid metabolism in regulation of macrophage functions. Trends in Cell

Biology, 30(12):979–989.

9. List of figures

10. List of tables